Commun. Comput. Phys.
doi: 10.4208/cicp.OA-2017-0204

Vol. **25**, No. 2, pp. 532-563
February 2019

Conservative and Dissipative Local Discontinuous Galerkin Methods for Korteweg-de Vries Type Equations

Qian Zhang[1] and Yinhua Xia[1,*]

[1] *School of Mathematical Sciences, University of Science and Technology of China, Hefei, Anhui 230026, P.R. China.*

Received 24 September 2017; Accepted (in revised version) 12 February 2018

Abstract. In this paper, we develop the Hamiltonian conservative and L^2 conservative local discontinuous Galerkin (LDG) schemes for the Korteweg-de Vries (KdV) type equations with the minimal stencil. For the time discretization, we adopt the semi-implicit spectral deferred correction (SDC) method to achieve the high order accuracy and efficiency. Also we compare the schemes with the dissipative LDG scheme. Stability of the fully discrete schemes is provided by Fourier analysis for the linearized KdV equation. Numerical examples are shown to illustrate the capability of these schemes. Compared with the dissipative LDG scheme, the numerical simulations also indicate that the conservative LDG scheme with high order time discretization can reduce the long time phase error validly.

AMS subject classifications: 65M60, 65M12, 35Q53

Key words: Local discontinuous Galerkin method, conservative and dissipative schemes, Korteweg-de Vries type equations, semi-implicit spectral deferred correction method.

1 Introduction

In this paper, we consider the initial value problem of Korteweg-de Vries (KdV) equation

$$\begin{cases} u_t + f(u)_x + \varepsilon u_{xxx} = 0, \ \ x \in I = [a,b], \ \ t > 0, \\ u(x,0) = u_0(x), \end{cases} \tag{1.1}$$

where t is time, x is the space coordinate in the direction of propagation, $a,b,\varepsilon \in \mathbb{R}, \varepsilon > 0$. With smooth enough initial condition $u_0(x)$, we can obtain the existence and uniqueness of solution [8]. The KdV equation is first introduced by Boussinesq (1877) and rediscovered by Diederik Korteweg and Gustav de Vries in 1895 [14], in which studies the

*Corresponding author. *Email addresses:* gelee@mail.ustc.edu.cn (Q. Zhang), yhxia@ustc.edu.cn (Y. Xia)

small-amplitude long waves in shallow water. In the study of water wave, it has two well-known solutions, cnoidal wave and solitary wave solutions. In the last decades, since the soliton solution proposed by Zabusky and Kruskal [33], the KdV equation has risen a considerable interest by physicists and mathematicians. Actually, the KdV equation is a mathematical model for the propagation of nonlinear dispersive long waves in many branches of physics and engineering including aerology, oceanography, plasma physic, geology, among many others.

Various numerical methods of solving this equation have been proposed, like finite-difference schemes [12, 20], pseudospectral methods [10], heat balance integral method [15] and finite element method, especially discontinuous Galerkin method. The discontinuous Galerkin method (DG method) is a class of finite element methods using completely discontinuous piecewise polynomial functions as numerical approximation and test functions. The DG method was first introduced in 1973 by Reed and Hill in [19] for solving steady state linear hyperbolic equations. The important ingredient of this method is the design of suitable inter-element boundary treatments (so called numerical fluxes) to obtain highly accurate and stable schemes in many situations.

Within the DG framework, the method was extended to deal with derivatives of order higher than one, i.e. local discontinuous Galerkin (LDG) method. The first LDG method was introduced by Cockburn and Shu in [5] for solving convection-diffusion equation. Their work was motivated by the successful numerical experiments of Bassi and Rebay [3] for compressible Navier-Stokes equations. Later, Yan and Shu developed a LDG numerical method for a general KdV type equation containing third order derivatives in [31], and they generalized the LDG method to PDEs with fourth and fifth spatial derivatives in [32]. Levy, Shu and Yan [17] developed LDG methods for nonlinear dispersive equations that have compactly supported traveling wave solutions, the so-called compactons. More recently, Xu and Shu further generalized the LDG method to solve a series of nonlinear wave equations [24–27]. We refer to the review paper [29] of LDG methods for high-order time-dependent partial differential equations.

According to the selection of numerical flux function for the nonlinear term $f(u)$ and the dispersive term εu_{xxx} in KdV equations, the DG method can be divided into dissipative and conservative schemes. Conservative discretization scheme means that this scheme can preserve certain conserved quantities discretely. In the numerical experiments of [4], the higher accuracy and better stability of the conservative scheme over long temporal intervals can be seen. Usually, the conservation of L^2 energy

$$H_1 = \int \frac{1}{2} u^2 dx, \tag{1.2}$$

and the conservation of the Hamiltonian

$$H_2 = \int \frac{\varepsilon}{2} u_x^2 - V(u) dx, \quad V(u) = \int^u f(\zeta)\, d\zeta, \tag{1.3}$$

are considered, since the KdV equation is a Hamiltonian system [11].

In [31], Yan and Shu proposed a dissipative LDG method for the KdV equation and proved the L^2 sub-optimal error estimates of the semi-discrete LDG numerical method for linear KdV equation. Then Xu and Shu proved the L^2 optimal semi-discrete error estimates for the linear KdV equation in [30]. Cheng and Shu developed a new discontinuous Galerkin method in [7] to solve KdV equation without the auxiliary variables in LDG numerical method. Based on the results of Cheng and Shu, Bona et al. proposed a global projection in [4] to develop conservative method for generalized KdV type equations. However, this method does not achieve the optimal $(k+1)$-th order of accuracy when piecewise polynomials of odd degree k is used (this accuracy degeneracy is well known for even k and is also shown to exist for odd k recently in [13]). In [16], the authors developed the L^2 conservative LDG numerical scheme and compared with dissipative LDG scheme for KdV type equations to display the phase error caused by dissipation. Compared with the dissipative scheme, the L^2 conservative in [16] and Hamiltonian conservative LDG numerical scheme proposed in [18] can both reduce the phase error efficiently. For even k, these L^2 and Hamiltonian conservative schemes can achieve optimal order of convergence rate, however, for odd k, only reach sub-optimal order. Meanwhile, the conservative LDG numerical schemes in [22, 23] for long wave and short wave interaction systems appear to have better convergence rate, due to the alternative numerical fluxes are adopted as much as possible. It results in the LDG scheme with the minimal stencil. In this paper we will develop the Hamiltonian conservative and L^2 conservative LDG schemes for KdV type equations with the minimal stencil. It likely has better accuracy for Hamiltonian conservation LDG scheme with the minimal stencil through the numerical experiments in Section 4.

To achieve the high order accuracy and efficiency for the fully discrete scheme, we adopt the spectral deferred correction (SDC) scheme [9]. It is based on low order time integration methods which are corrected iteratively, with the order of accuracy increased for each additional iteration. Due to the third derivative term, explicit time discretization will suffer from a strict time step restriction for stability. Implicit time discretization like mid-point time discretization scheme can break the time step restriction. Combined with conservative spatial discretization scheme, it can achieve a conservative fully discrete scheme which can reduce phase error. However, for nonlinear term $f(u)$, implicit scheme associated with a nonlinear algebraic system will cause computation complication. Thus, semi-implicit SDC scheme is used to solve the KdV type equation in [21] to achieve arbitrary high order accuracy and efficiency. For nonlinear term, we use explicit time discretization while using implicit time discretization for the third order derivative term. When high order semi-implicit SDC schemes combine with conservative LDG numerical schemes, it can reduce the phase error efficiently even though the fully discrete scheme is no longer conservative.

The paper is organized as follows. In Section 2, we introduce the LDG numerical method briefly. Combining with different numerical flux functions, we present L^2 conservative LDG numerical scheme and Hamiltonian conservative LDG numerical scheme respectively. Section 3 is devoted to time discretization methods, especially the semi-

implicit SDC scheme and the Fourier stability analysis of the fully discrete schemes for the linearized KdV equation. And in Section 4 we provide a few numerical experiments which include linear and nonlinear KdV equations to illustrate the accuracy and the long time behavior of the dissipative and conservative LDG schemes. Concluding remarks are given in Section 5.

2 Conservative local discontinuous Galerkin method

In this section, we present and analyze the L^2 and Hamiltonian conservative local discontinuous Galerkin schemes for the KdV equation (1.1) with the period L. Notice that the assumption of periodic boundary conditions is for simplicity only and is not essential. The method can be easily designed for non-periodic boundary conditions.

We denote the mesh $\mathcal{T}_h$ by $I_j=[x_{j-\frac{1}{2}},x_{j+\frac{1}{2}}]$ for $j=1,\cdots,N$, with the cell center denoted by $x_j=\frac{1}{2}(x_{j-\frac{1}{2}}+x_{j+\frac{1}{2}})$. The cell size is $\Delta x_j=x_{j+\frac{1}{2}}-x_{j-\frac{1}{2}}$ and $h=\max_{1\le j\le N}\Delta x_j$. We define the finite element space as the solution and test function space consisting of piecewise polynomials

$$V_h^k=\{v\colon v|_{I_j}\in P^k(I_j);\ 1\le j\le N\},$$

where $P^k(I_j)$ denotes the set of polynomial of degree up to k defined on the cell I_j. Note that functions in V_h^k are allowed to have discontinuous across cell interfaces. We also denote by the $u^-_{j+\frac{1}{2}}$ and $u^+_{j+\frac{1}{2}}$ the values of u at $x_{j+\frac{1}{2}}$, from the left cell I_j and the right cell I_{j+1} respectively. And we define the jump of u as $[[u]]=u^+-u^-$, the average of u as $\{\{u\}\}=\frac{1}{2}(u^++u^-)$. For simplicity, we just set $\varepsilon=1$ in the description of Section 2 and Section 3.

Following the framework of LDG numerical method [29], we first rewrite the KdV equation (1.1) as a first-order system:

$$\begin{cases} u_t+f(u)_x+w_x=0, \\ w-v_x=0, \\ v-u_x=0. \end{cases} \tag{2.1}$$

Then the LDG scheme to the solve the first-order KdV system (2.1) is as follows: find u_h, w_h and $v_h\in V_h^k$ such that

$$\begin{cases} ((u_h)_t,\phi)_{I_j}+<\widehat{f(u_h)},\phi>_{I_j}-(f(u_h),\phi_x)_{I_j}+<\widehat{w_h},\phi>_{I_j}-(w_h,\phi_x)_{I_j}=0, \\ (w_h,\varphi)_{I_j}-<\widehat{v_h},\varphi>_{I_j}+(v_h,\varphi_x)_{I_j}=0, \\ (v_h,\psi)_{I_j}-<\widehat{u_h},\psi>_{I_j}+(u_h,\psi_x)_{I_j}=0, \end{cases} \tag{2.2}$$

for all test functions $\phi,\varphi,\psi\in V_h^k$, and $I_j\in\mathcal{T}_h$. Here, we adopt the round bracket and angle

bracket to simplify the expressions:

$$\begin{aligned}&(u,v)_{I_j}=\int_{I_j}uvdx,\\&<\hat{u},v>_{I_j}=\hat{u}_{j+\frac{1}{2}}v^-_{j+\frac{1}{2}}-\hat{u}_{j-\frac{1}{2}}v^+_{j-\frac{1}{2}},\end{aligned}\tag{2.3}$$

for one dimension case. The "hat" terms in (2.2) are the so-called numerical fluxes which are functions defined on the cell boundary from integration by parts and should be designed based on different guiding principles for different PDEs to ensure stability and local solvability of the intermediate variables.

We introduce the following operators to simplify our notations:

Definition 2.1. We define the operators $L_j^{\pm,c}(\cdot,\cdot)$ as follows:

$$L_j^+(u,v)=-(u,v_x)_{I_j}+<u^+,v>_{I_j},\tag{2.4}$$

$$L_j^-(u,v)=-(u,v_x)_{I_j}+<u^-,v>_{I_j},\tag{2.5}$$

$$L_j^c(u,v)=-(u,v_x)_{I_j}+<\{\{u\}\},v>_{I_j}\tag{2.6}$$

for $\forall u,v\in V_h^k$.

Definition 2.2. The operators $N_j^{c,d}(\cdot,\cdot)$ for the nonlinear term $f(u)$ of KdV equation are defined:

$$N_j^d(u,\phi)=-(f(u),\phi_x)_{I_j}+<\widehat{f(u)},\phi>_{I_j},\tag{2.7}$$

where $\widehat{f(u)}=\frac{1}{2}(f(u^+)+f(u^-)-\alpha(u^+-u^-))$, $\alpha=\max_u|f'(u)|$, it is dissipative treatment for the nonlinear term. Then we define the conservative treatment for $f(u)$

$$N_j^c(u,\phi)=-(f(u),\phi_x)_{I_j}+<\widehat{f(u)},\phi>_{I_j},\tag{2.8}$$

where $\widehat{f(u)}$ is taken as conservative flux function

$$\widehat{f(u)}=\begin{cases}\frac{[[F(u)]]}{[[u]]}, & [[u]]\neq 0,\\ f(\{\{u\}\}), & [[u]]=0.\end{cases},\tag{2.9}$$

where $F(u)=\int^u f(\tau)d\tau$, especially for $f(u)=u^p$, p is integer,

$$\widehat{f(u)}=\frac{1}{p+1}\sum_{j=0}^{p}(u^+)^{p-j}(u^-)^j,$$

for $\forall u,v\in V_h^k$ as in [4].

Lemma 2.1. *Let* $L^{\pm,c}=\sum_j L_j^{\pm,c}$, $N^{c,d}=\sum_j N_j^{c,d}$, *there holds the equalities*

$$L^c(u,u)=0, \tag{2.10}$$

$$L^-(u,u)=\frac{1}{2}[[u]]^2, \tag{2.11}$$

$$L^+(u,v)=-L^-(v,u), \tag{2.12}$$

$$L^c(u,v)=-L^c(v,u), \tag{2.13}$$

$$N^d(u,u)\geq 0, \tag{2.14}$$

$$N^c(u,u)=0, \tag{2.15}$$

for $\forall u,v\in V_h^k$.

These properties in Lemma (2.1) are listed in [28], [4], so we do not give the detail here.

Then the dissipative LDG numerical scheme in [31] could be written as

$$\begin{cases}((u_h)_t,\phi)_{I_j}+N_j^d(u_h,\phi)+L_j^+(w_h,\phi)=0,\\ (w_h,\varphi)_{I_j}-L_j^+(v_h,\varphi)=0,\\ (v_h,\psi)_{I_j}-L_j^-(u_h,\psi)=0,\end{cases} \tag{2.16}$$

which can also be written as the scheme (2.2) with the numerical fluxes

$$\widehat{w_h}=w_h^+,\quad \widehat{v_h}=v_h^+,\quad \widehat{u_h}=u_h^- \tag{2.17}$$

and $\widehat{f(u)}$ in (2.7). Here, we remark that the numerical fluxes we take above are not unique. The key for third derivative term is the opposite sides between $\widehat{u_h}$ and $\widehat{w_h}$. $\widehat{v_h}$ depends on the sign of ε. We assume that $\varepsilon>0$ in this paper, then for dissipative numerical fluxes, $\widehat{v_h}$ should be taken as v_h^+. For the nonlinear term $f(u)$, flux function for the dissipative LDG numerical scheme can also be Godunov, Boltzmann and Engquist-Osher flux function.

In [31], the dissipative LDG numerical fluxes have been adopted for KdV equation. For hyperbolic conservation laws, the dissipative numerical fluxes are chosen such that the entropy condition can be satisfied. As an additional condition, entropy condition leads us to single out entropy solution among the infinitely weak solutions. Analogously, the dissipation introduced by the LDG numerical scheme for the KdV type equation is essential to ensure stability for the odd derivatives which correspond to waves. However, the KdV type equation profiles the propagation of nonlinear, dispersive waves which cause the energy conservation of general initial data. The dissipative LDG numerical scheme will destroy the balance between nonlinear steepening and dispersive spreading. Numerically, it will cause the phase error, shape error and the inaccuracy of the LDG numerical scheme over a long temporal interval. In [4], [16], [18], the authors developed

some different kinds of conservative schemes (details will be discussed presently) for the KdV type equation. The conservative scheme means that it can preserve the conserved quantities discretely so that the numerical schemes can approximate the conservative form of the KdV equation. Comparing with the dissipative scheme, the conservative discretization scheme not only has high accuracy and good stability, but reduces the phase error and shape error validly over a long temporal interval, especially in low order approximation.

Proposition 2.1. (L^2 stability for the dissipative scheme (2.16)) First, we give the cell entropy inequality

$$\frac{d}{dt}\int_K \frac{u_h^2(x,t)}{2}dx+\hat{F}_{j+\frac{1}{2}}-\hat{F}_{j-\frac{1}{2}}\leq 0, \tag{2.18}$$

where numerical entropy flux $\hat{F}_{j+\frac{1}{2}}$ is

$$\hat{F}_{j+\frac{1}{2}}=\hat{F}\Big(u_h(x^-_{j+\frac{1}{2}},t),\, w_h(x^-_{j+\frac{1}{2}},t),\, v_h(x^-_{j+\frac{1}{2}},t),\, u_h(x^+_{j+\frac{1}{2}},t),\, w_h(x^+_{j+\frac{1}{2}},t),\, v_h(x^+_{j+\frac{1}{2}},t)\Big). \tag{2.19}$$

Adding up (2.18) over all $I_j\in\mathcal{T}_h$, we have L^2 stability

$$\sum_j((u_h)_t,u_h)_{I_j}\leq 0. \tag{2.20}$$

The entropy inequality and stability of the dissipative LDG numerical scheme for the KdV type equation are mentioned in [31], in which the L^2 sub-optimal error estimate of the semi-discrete dissipative LDG numerical scheme for the linear KdV type equation have been proved. In [30], Xu and Shu proved the L^2 optimal semi-discrete error estimate of the dissipative LDG numerical scheme for the linear KdV type equation.

We denote this dissipative LDG numerical scheme by NC-NC scheme in the section of numerical experiments, which means we treat nonlinear term $f(u)$ and third derivative term both non-conservative.

2.1 L^2 Conservative LDG numerical scheme

To construct a L^2 conservative LDG numerical scheme, we choose the following numerical fluxes in (2.2)

$$\widehat{f(u)}=\begin{cases}\frac{[[F(u)]]}{[[u]]}, & [[u]]\neq 0,\\ f(\{\{u\}\}), & [[u]]=0,\end{cases}\quad \widehat{w_h}=w_h^-,\quad \widehat{v_h}=\{\{v_h\}\},\quad \widehat{u_h}=u_h^+ \tag{2.21}$$

as a replacement, we could also take

$$\widehat{f(u)}=\begin{cases}\frac{[[F(u)]]}{[[u]]}, & [[u]]\neq 0,\\ f(\{\{u\}\}), & [[u]]=0,\end{cases}\quad \widehat{w_h}=w_h^+,\quad \widehat{v_h}=\{\{v_h\}\},\quad \widehat{u_h}=u_h^-, \tag{2.22}$$

where

$$F(u)=\int^{u} f(\tau)d\tau. \tag{2.23}$$

The main differences between the numerical fluxes (2.21) and Karakashian and Xing [16], Liu and Yi [18], are the choice of $\widehat{w_h}$ and $\widehat{u_h}$. According to our notations, their numerical fluxes of L^2 conservative LDG numerical scheme can be presented as

$$\widehat{f(u)}=\begin{cases}\frac{[[F(u)]]}{[[u]]}, & [[u]]\neq 0,\\ f(\{\{u\}\}), & [[u]]=0,\end{cases}\quad \widehat{w_h}=\{\{w_h\}\},\quad \widehat{v_h}=\{\{v_h\}\},\quad \widehat{u_h}=\{\{u_h\}\}. \tag{2.24}$$

With these numerical fluxes (2.21), Eq. (2.2) can be rewritten as

$$\begin{cases}((u_h)_t,\phi)_{I_j}+N_j^c(u_h,\phi)+L_j^+(w_h,\phi)=0,\\ (w_h,\varphi)_{I_j}-L_j^c(v_h,\varphi)=0,\\ (v_h,\psi)_{I_j}-L_j^-(u_h,\psi)=0,\end{cases} \tag{2.25}$$

for all test functions $\phi,\varphi,\psi\in V_h^k$, and $I_j\in\mathcal{T}_h$.

Proposition 2.2. We get the L^2 conservative LDG numerical scheme (2.25). The following equality can be established

$$\sum_j((u_h)_t,u_h)_{I_j}=0,$$

that is, H_1 in (1.2) is a conservative quantity numerically.

Proof. By choosing $\phi=u_h,\varphi=v_h$ and $\psi=-w_h$ in the scheme (2.25), we have

$$\begin{aligned}&((u_h)_t,u_h)_{I_j}+N_j^c(u_h,u_h)+L_j^+(w_h,u_h)=0,\\ &(w_h,v_h)_{I_j}-L_j^c(v_h,v_h)=0,\\ &-(v_h,w_h)_{I_j}+L_j^-(u_h,w_h)=0.\end{aligned}$$

After summation over $I_j\in\mathcal{T}_h$, we can get

$$\sum_j N_j^c(u_h,u_h)+L_j^+(w_h,u_h)+L_j^-(u_h,w_h)+L_j^c(v_h,v_h)=0.$$

By Lemma 2.1, we obtain

$$\sum_j((u_h)_t,u_h)_{I_j}=0.$$

The proof is completed. □

We denote this L^2 conservative LDG numerical scheme by C-C scheme. For L^2 conservative LDG numerical scheme with numerical fluxes (2.24), L^2 optimal error estimates are obtained for the linear KdV equation in [16, 18] when k is even and N is odd. More generally, the L^2 conservative numerical fluxes can be defined as $\widehat{w_h}=\{\{w_h\}\}+\alpha[[w_h]]$ and $\widehat{u_h}=\{\{u_h\}\}-\alpha[[u_h]]$ in (2.21). When $\alpha\neq\pm\frac{1}{2}$, it results a wider stencil LDG scheme than the scheme (2.25).

To compare the differences among spatial discretization schemes, we introduce NC-C scheme which treats $f(u)$ non-conservative and the third derivative term εu_{xxx} conservative. The semi-discrete LDG numerical scheme can be written as

$$\begin{cases}((u_h)_t,\phi)_{I_j}+N_j^d(u_h,\phi)+L_j^+(w_h,\phi)=0,\\(w_h,\varphi)_{I_j}-L_j^c(v_h,\varphi)=0,\\(v_h,\psi)_{I_j}-L_j^-(u_h,\psi)=0,\end{cases}\tag{2.26}$$

for all test functions $\phi,\varphi,\psi\in V_h^k$, and $I_j\in\mathcal{T}_h$. It is obvious that this NC-C scheme is also dissipative.

2.2 Hamiltonian conservative LDG numerical scheme

In this section, we introduce the Hamiltonian conservative LDG numerical scheme. In [18], Liu and Yi presented a Hamiltonian conservative LDG numerical scheme for the KdV type equation. First we rewrite the KdV equation (1.1) into a first order system

$$\begin{cases}u_t+p_x+w_x=0,\\w-v_x=0,\\v-u_x=0,\\p-f(u)=0.\end{cases}\tag{2.27}$$

Then the semi-discrete Hamiltonian conservative LDG numerical scheme is defined: find u_h, w_h, and $v_h\in V_h^k$ such that

$$\begin{cases}((u_h)_t,\phi)_{I_j}-L_j^c(w_h,\phi)=0,\\(w_h,\varphi)_{I_j}+L_j^c(v_h,\varphi)+(f(u_h),\varphi)_{I_j}=0,\\(v_h,\psi)_{I_j}-L_j^c(u_h,\psi)=0,\end{cases}\tag{2.28}$$

for all test functions $\phi,\varphi,\psi\in V_h^k$, and $I_j\in\mathcal{T}_h$. For this LDG numerical scheme, the conserved quantity H_2 is conservative numerically. Unlike the above scheme (2.28), we adopt different numerical fluxes as follows:

$$\widehat{p_h}=\{\{p_h\}\},\quad \widehat{w_h}=\{\{w_h\}\},\quad \widehat{v_h}=v_h^-,\quad \widehat{u_h}=u_h^+.\tag{2.29}$$

Then the semi-discrete Hamiltonian conservative LDG numerical scheme is defined as: find u_h, w_h, v_h and $p_h \in V_h^k$ such that

$$\begin{cases} ((u_h)_t,\phi)_{I_j}+L_j^c(p_h,\phi)+L_j^c(w_h,\phi)=0, \\ (w_h,\varphi)_{I_j}-L_j^-(v_h,\varphi)=0, \\ (v_h,\psi)_{I_j}-L_j^+(u_h,\psi)=0, \\ (p_h,\eta)_{I_j}-(f(u_h),\eta)_{I_j}=0, \end{cases} \tag{2.30}$$

for all test functions $\phi,\varphi,\psi,\eta \in V_h^k$, and $I_j \in \mathcal{T}_h$.

Proposition 2.3. For Hamiltonian conservative LDG numerical scheme (2.30), there holds an equality

$$\sum_j ((v_h)_t,v_h)_{I_j}-(f(u_h),(u_h)_t)_{I_j}=0, \tag{2.31}$$

that is, H_2 in (1.3) is a conservative quantity numerically.

Proof. Let $q_h \in V_h^k$, such that

$$\begin{cases} L_j^c(q_h,\xi)=(u_h,\xi)_{I_j}, \\ \int_I q_h dx=0 \end{cases} \tag{2.32}$$

for all test functions $\xi \in V_h$, and $I_j \in \mathcal{T}_h$. Taking the time derivative of (2.32) and Choosing $\xi=p_h,w_h$ and $(q_h)_t$ in (2.32) respectively, we obtain

$$\begin{aligned} &L_j^c((q_h)_t,p_h)=((u_h)_t,p_h)_{I_j}, \\ &L_j^c((q_h)_t,w_h)=((u_h)_t,w_h)_{I_j}, \\ &L_j^c((q_h)_t,(q_h)_t)=((u_h)_t,(q_h)_t))_{I_j}. \end{aligned} \tag{2.33}$$

Taking the time derivative of the third equation of (2.30) and $\phi=(q_h)_t$, $\varphi=(u_h)_t$, $\psi=v_h$, $\eta=(u_h)_t$, we have

$$\begin{aligned} &((u_h)_t,(q_h)_t)_{I_j}+L_j^c(p_h,(q_h)_t)+L_j^c(w_h,(q_h)_t)=0, \\ &(w_h,(u_h)_t)_{I_j}-L_j^-(v_h,(u_h)_t)=0, \\ &((v_h)_t,v_h)_{I_j}-L_j^+((u_h)_t,v_h)=0, \\ &(p_h,(u_h)_t)_{I_j}-(f(u_h),(u_h)_t)_{I_j}=0. \end{aligned} \tag{2.34}$$

Summing up all equalities in (2.34) over $I_j \in \mathcal{T}_h$, we get

$$\begin{aligned} \sum_j &((u_h)_t,(q_h)_t)_{I_j}+L_j^c(p_h,(q_h)_t)+((u_h)_t,p_h)_{I_j} \\ &+L_j^c(w_h,(q_h)_t)+((u_h)_t,w_h)_{I_j}-(L_j^+((u_h)_t,v_h)+L_j^-(v_h,(u_h)_t)) \\ &+(v_h,(v_h)_t)_{I_j}-(f(u_h),(u_h)_t)_{I_j}=0. \end{aligned} \tag{2.35}$$

Finally, according to the equalities (2.33) and Lemma 2.1, we obtain

$$\sum_j ((v_h)_t, v_h)_{I_j} - (f(u_h), (u_h)_t)_{I_j} = 0. \tag{2.36}$$

The proof is completed. □

We denote the Hamiltonian conservative LDG numerical scheme by HC scheme. For the linear KdV equation, the schemes in [16, 18] are the same. To obtain the Hamiltonian conservation, numerical fluxes $\widehat{v_h}$ and $\widehat{u_h}$ in (2.29) can also chosen as $\widehat{v_h} = \{\{v_h\}\} + \alpha[[v_h]]$ and $\widehat{u_h} = \{\{u_h\}\} - \alpha[[u_h]]$, which results a wider stencil LDG scheme than the scheme (2.30) when $\alpha \neq \pm\frac{1}{2}$.

3 Time discretization

In this section, we mainly utilize semi-implicit SDC schemes. The initial value problem for a first-order system of ODEs takes the form

$$\begin{cases} u_t = F_E(t, u(t)) + F_I(t, u(t)), & t \in [0, T], \\ u(0) = u_0, \end{cases} \tag{3.1}$$

where F_E is a non-stiff term and F_I is a stiff term. The subscripts refer that the non-stiff term is treated explicitly and the stiff term is treated implicitly. For the KdV type equation (1.1)

$$F_E = f(u)_x; \quad F_I = \varepsilon u_{xxx}; \quad F \triangleq F_E + F_I, \tag{3.2}$$

resulting a linear implicit scheme.

We divide the temporal interval [0,T] into N subintervals, $0 = t_0 < t_1 < \cdots < t_n < \cdots < t_N = T$. And we denote $\Delta t_n = t_{n+1} - t_n$. u_n is the numerical approximation of $u(t_n)$ and $u_0 = u(0)$.

3.1 Semi-implicit SDC scheme

The spectral deferred correction method (SDC) was presented by Dutt, Greengard and Rokhlin in [9]. It is based on low order time integration methods which are corrected iteratively, with the order of accuracy increased for each additional iteration. In [21], Xia et al. developed three different time discretization schemes including semi-implicit SDC scheme for solving the stiff ODEs resulting from a LDG spatial discretization to PDEs containing high order spatial derivatives. Semi-implicit implies that we will split stiff and non-stiff terms as needed, and discretize implicitly for the stiff terms and explicitly for the non-stiff terms. This treatment enlarges time steps $\Delta t = \mathcal{O}(\Delta x)$ rather than the much more restrictive $\Delta t = \mathcal{O}(\Delta x^k)$ of explicit time discretization for k-th order PDEs.

Also, the linear implicit scheme reduces the complexity of computation comparing to the nonlinear implicit scheme.

We rewrite the equation (3.1) into an integral form in the subinterval $[t_n,t_{n+1}]$:

$$u(t_{n+1})=u(t_n)+\int_{t_n}^{t_{n+1}}F(\tau,u(\tau))d\tau. \tag{3.3}$$

In $[t_n,t_{n+1}]$, choosing the points $t_{n,m}$ for $m=0,1,\cdots,P$ such that

$$t_n=t_{n,0}<t_{n,1}<\cdots<t_{n,m}<\cdots<t_{n,P}=t_{n+1}, \tag{3.4}$$

$$\Delta t_{n,m}=t_{n,m+1}-t_{n,m},\quad u_{n,m}^k\simeq u(t_{n,m}), \tag{3.5}$$

where $u_{n,m}^k$ is the *k-th* order approximation to $u(t_{n,m})$. Generally, we choose the Gauss-Lobatto nodes as $t_{n,m}$ in $[t_n,t_{n+1}]$. Gauss-Legendre, Gauss-Radau or Chebyshev nodes can be also used to avoid the instability of approximation at equispaced nodes for high order accuracy.

The algorithm is given as following:

We use the forward/backward Euler method for non-stiff/stiff terms to compute an approximation solution $u^1(t_{n,m})$, $m=0,\cdots,P$.

$$\begin{aligned}
&u_{n,0}^1=u_n.\\
&\text{For}\, m=0,\cdots P-1\\
&\quad u_{n,m+1}^1=u_{n,m}^1+\Delta t_{n,m}F_E(t_{n,m},u_{n,m}^1)+\Delta t_{n,m}F_I(t_{n,m+1},u_{n,m+1}^1).\\
&\text{End for}
\end{aligned} \tag{3.6}$$

Then we compute the successive corrections

$$\begin{aligned}
&\text{For}\, k=1,\cdots,K\\
&\quad u_{n,0}^{k+1}=u_n.\\
&\quad \text{For}\, m=0,\cdots P-1\\
&\quad u_{n,m+1}^{k+1}=u_{n,m}^{k+1}+\theta_1\Delta t_{n,m}(F_E(t_{n,m},u_{n,m}^{k+1})-F_E(t_{n,m},u_{n,m}^k))\\
&\qquad\quad +\theta_2\Delta t_{n,m}(F_I(t_{n,m+1},u_{n,m+1}^{k+1})-F_I(t_{n,m+1},u_{n,m+1}^k))+I_m^{m+1}(F(t,u^k)).\\
&\quad \text{End for}\\
&\text{End for}\\
&u_{n+1}=u_{n,P}^{K+1}
\end{aligned} \tag{3.7}$$

where $0\le\theta_1,\theta_2\le 1$. In Section 4, we adopt $\theta_1=0$, $\theta_2=1$ mostly. There is a few comments on the form of the quadrature for $I_m^{m+1}(F(t,u^k))$. The points $t_{n,m}$ lies in the interior of the interval $[t_n,t_{n+1}]$, the quadrature must be done for each $[t_m,t_{m+1}]$, there are P quadrature rules

$$I_m^{m+1}(F(t,u^k))=\sum_{l=0}^{P}q_m^lF(t_l,u_l^k),\quad m=1,\cdots,P-1. \tag{3.8}$$

We can precomputed the coefficients q_m^l, and the quadrature is reduced to a simple matrix-vector multiplication.

3.2 Fourier analysis of fully discrete schemes

After the introduction of space and time discretization, we attempt to give an stability analysis of fully discrete scheme for linear KdV equation

$$u_t+u_x+u_{xxx}=0. \tag{3.9}$$

Fourier expansion method in [34] can be used to analyze the stability. Above four schemes in Section 2 are semi-discrete schemes, i.e. the conservativeness is a spatial property. Time discretization need to be added to analyze the fully discrete scheme and fully conservativeness. But as a result of non-conservativeness of semi-implicit SDC time discretization method, generally, the fully discrete schemes are not completely conservative. So these four schemes have different degrees of dissipation or ascent which can have some effect on the numerical results. To compare, we also list a conservative time discretization scheme called mid-point scheme [4]. Combining with C-C spatial discretization scheme, we get a L^2 conservative fully discrete scheme. In Section 4, we also list a few results that use IMEX Runge-Kutta schemes [2] as time discretization scheme.

First, we need rewrite the formulation of the LDG numerical scheme as finite difference scheme, and then we use finite difference techniques to analyze stability. Towards this goal we choose the degrees of freedom for the k-th degree polynomial inside the cell I_j as the point values of solution, denoted by

$$u_{j+\frac{2i-k}{2(k+1)}}, \quad i=0,\cdots,k, \tag{3.10}$$

at the $k+1$ equally spaced nodes

$$\left(j+\frac{2i-k}{2(k+1)}\right)\Delta x, \quad i=0,\cdots,k. \tag{3.11}$$

According to these degrees of freedom, the discontinuous Galerkin method become finite difference scheme on a global uniform mesh with a mesh size $\Delta x/(k+1)$. We take $k=1$ as a example, the degrees of freedom are the value of spaced node

$$u_{j-\frac{1}{4}},u_{j+\frac{1}{4}}, \quad j=1,\cdots,N. \tag{3.12}$$

Solution inside the cell I_j is represented by

$$u(x)=u_{j-\frac{1}{4}}\phi_{j-\frac{1}{4}}+u_{j+\frac{1}{4}}\phi_{j+\frac{1}{4}}, \tag{3.13}$$

where

$$\begin{aligned} &\phi_{j-\frac{1}{4}}(x_{j-\frac{1}{4}})=1, \quad \phi_{j-\frac{1}{4}}(x_{j+\frac{1}{4}})=0,\\ &\phi_{j+\frac{1}{4}}(x_{j-\frac{1}{4}})=0, \quad \phi_{j+\frac{1}{4}}(x_{j+\frac{1}{4}})=1. \end{aligned} \tag{3.14}$$

We take the test functions also as $\phi_{j-\frac{1}{4}}(x)$ and $\phi_{j+\frac{1}{4}}(x)$, then we obtain easily the finite difference scheme.

We rewrite the NC-NC scheme(2.16) in matrix form

$$\begin{aligned}
&M\begin{pmatrix} v_{j-\frac{1}{4}} \\ v_{j+\frac{1}{4}} \end{pmatrix} = \frac{1}{\Delta x}\left[A_1\begin{pmatrix} u_{j-\frac{1}{4}} \\ u_{j+\frac{1}{4}} \end{pmatrix} + B_1\begin{pmatrix} u_{j-\frac{5}{4}} \\ u_{j-\frac{3}{4}} \end{pmatrix}\right], \\
&M\begin{pmatrix} w_{j-\frac{1}{4}} \\ w_{j+\frac{1}{4}} \end{pmatrix} = \frac{1}{\Delta x}\left[A_2\begin{pmatrix} v_{j-\frac{1}{4}} \\ v_{j+\frac{1}{4}} \end{pmatrix} + B_2\begin{pmatrix} v_{j+\frac{3}{4}} \\ v_{j+\frac{5}{4}} \end{pmatrix}\right], \\
&M\begin{pmatrix} u'_{j-\frac{1}{4}} \\ u'_{j+\frac{1}{4}} \end{pmatrix} = -\frac{1}{\Delta x}\left[A_1\begin{pmatrix} u_{j-\frac{1}{4}} \\ u_{j+\frac{1}{4}} \end{pmatrix} + B_1\begin{pmatrix} u_{j-\frac{5}{4}} \\ u_{j-\frac{3}{4}} \end{pmatrix}\right] - \frac{1}{\Delta x}\left[A_2\begin{pmatrix} w_{j-\frac{1}{4}} \\ w_{j+\frac{1}{4}} \end{pmatrix} + B_2\begin{pmatrix} w_{j+\frac{3}{4}} \\ w_{j+\frac{5}{4}} \end{pmatrix}\right]
\end{aligned} \tag{3.15}$$

for $j=1,\cdots,N$. Here we denote the time derivative of u by u', M denotes mass matrix. And A_1,B_1 denote the coefficient matrixes of numerical flux L_j^- and the integral term, respectively; A_2,B_2 denote those of numerical flux L_j^+ and the integral term, respectively.

$$\begin{aligned}
&A_1 = \begin{pmatrix} \frac{5}{4} & \frac{1}{4} \\ -\frac{7}{4} & \frac{5}{4} \end{pmatrix}, \quad B_1 = \begin{pmatrix} \frac{3}{4} & -\frac{9}{4} \\ -\frac{1}{4} & \frac{3}{4} \end{pmatrix}, \\
&A_2 = \begin{pmatrix} -\frac{5}{4} & \frac{7}{4} \\ -\frac{1}{4} & -\frac{5}{4} \end{pmatrix}, \quad B_2 = \begin{pmatrix} -\frac{3}{4} & \frac{1}{4} \\ \frac{9}{4} & -\frac{3}{4} \end{pmatrix}, \quad M = \Delta x\begin{pmatrix} \frac{7}{12} & -\frac{1}{12} \\ -\frac{1}{12} & \frac{7}{12} \end{pmatrix}.
\end{aligned}$$

We can write (3.15) into a more compact form

$$\begin{aligned}
\begin{pmatrix} u'_{j-\frac{1}{4}} \\ u'_{j+\frac{1}{4}} \end{pmatrix} =& -\left(\tfrac{1}{\Delta x}\right) M^{-1}\left[A_1\begin{pmatrix} u_{j-\frac{1}{4}} \\ u_{j+\frac{1}{4}} \end{pmatrix} + B_1\begin{pmatrix} u_{j-\frac{5}{4}} \\ u_{j-\frac{3}{4}} \end{pmatrix}\right] \\
&-\left(\tfrac{1}{\Delta x}\right)^3 M^{-1}\left[P_1\begin{pmatrix} u_{j+\frac{7}{4}} \\ u_{j+\frac{9}{4}} \end{pmatrix} + P_2\begin{pmatrix} u_{j+\frac{3}{4}} \\ u_{j+\frac{5}{4}} \end{pmatrix} + P_3\begin{pmatrix} u_{j-\frac{1}{4}} \\ u_{j+\frac{1}{4}} \end{pmatrix} + P_4\begin{pmatrix} u_{j-\frac{5}{4}} \\ u_{j-\frac{3}{4}} \end{pmatrix}\right],
\end{aligned} \tag{3.16}$$

where P_1,P_2,P_3,P_4 are the product of A_1,A_2,B_1,B_2. For (3.16), Fourier analysis can be used to prove stability. We make an ansatz of the form

$$\begin{pmatrix} u^n_{j-\frac{1}{4}}(t) \\ u^n_{j+\frac{1}{4}}(t) \end{pmatrix} = \begin{pmatrix} \hat{u}^n_{m,-\frac{1}{4}}(t) \\ \hat{u}^n_{m,\frac{1}{4}}(t) \end{pmatrix} e^{imx_j}, \tag{3.17}$$

and substitute this form into the (3.16) and we can get

$$\begin{pmatrix} \hat{u}'_{m,-\frac{1}{4}}(t) \\ \hat{u}'_{m,\frac{1}{4}}(t) \end{pmatrix} = G(m,\Delta x)\begin{pmatrix} \hat{u}_{m,-\frac{1}{4}}(t) \\ \hat{u}_{m,\frac{1}{4}}(t) \end{pmatrix}, \tag{3.18}$$

where $G(m,\Delta x)$ is called the amplification factor matrix, m is a integer which denotes frequency (or wavenumber) of wave. And then we consider the fully discrete scheme, for

u_t, we take Euler backward/forward time discretization method as a example to explain how to get the amplification factor matrix $G(m,\Delta x)$

$$\frac{u^{n+1}-u^n}{\Delta t}=F_E(u^n)+F_I(u^{n+1}), \tag{3.19}$$

where $F_E(u)=u_x$ and $F_I(u)=u_{xxx}$. We obtain

$$G(m,\Delta x)=\frac{I-\frac{\Delta t}{\Delta x}M^{-1}(A_1+B_1e^{-im\Delta x})}{I+\frac{\Delta t}{\Delta x^3}M^{-1}(P_1e^{2im\Delta x}+P_2e^{im\Delta x}+P_3+P_4e^{-im\Delta x})}. \tag{3.20}$$

For $k=1$, $G(m,\Delta x)$ is a 2×2 matrix. And we can obtain a conclusion about stability by comparing the absolute value of eigenvalue of the amplification factor matrix with 1. For C-C scheme, HC scheme and NC-C scheme, these schemes can be treated in the same way to obtain the amplification factor matrix. We denote the absolute value of eigenvalue of amplification factor matrix by G_1, G_2, G_3, G_4 for NC-NC, NC-C, C-C and HC schemes respectively. Without causing misunderstanding, we call G_i as amplification factor in the following description.

We compare G_i of some different schemes in Table 1, Figs. 1-4. Here, We take $\theta_1=0$, $\theta_2=\frac{2}{3}$ which we use in Section 4 to avoid instability. We notice that the stability varies with frequency of wave. When $\cos(m\Delta x)$ is close to 1, the amplification factors approximate to 1. The amplification factor of conservative fully discrete scheme in Fig. 2 have a upper bound $1+\mathcal{O}(10^{-14})$. When we choose semi-implicit SDC scheme as time discretization scheme, the differences between G_i and 1 can also be controlled by small quantity in Table 1. Although G_i is slightly larger than 1, it does not influence stability of numerical approximation schemes.

Table 1: The amplification factors G_i, $i=1,2,3,4$. $\theta_1=0$, $\theta_2=\frac{2}{3}$.

N	P_0 & Euler backward/forward	P^1 & SDC2	P^1 & mid-point	P^2 & SDC3
40	$G_i\leq 1$, $i=1,2,3,4$	$G_1<1$ $G_i\leq 1$, $i=1,2,3,4$	$G_1=1+\mathcal{O}(10^{-14})$ $G_2\leq 1$ $G_3=1+\mathcal{O}(10^{-14})$ $G_4=1+\mathcal{O}(10^{-14})$	$G_1=1+\mathcal{O}(10^{-10})$ $G_2=1+\mathcal{O}(10^{-8})$ $G_3=1+\mathcal{O}(10^{-8})$ $G_4=1+\mathcal{O}(10^{-8})$
80	$G_i\leq 1$, $i=1,2,3,4$	$G_1=1+\mathcal{O}(10^{-13})$ $G_i\leq 1$, $i=1,2,3,4$	$G_1=1+\mathcal{O}(10^{-15})$ $G_2\leq 1$ $G_3=1+\mathcal{O}(10^{-14})$ $G_4=1+\mathcal{O}(10^{-14})$	$G_1=1+\mathcal{O}(10^{-13})$ $G_i<1$, $i=1,2,3,4$

4 Numerical experiments

In this section, we test four kinds of spatial discretization schemes NC-NC, NC-C, C-C and HC schemes, which are defined in Section 2. The numerical results of the following

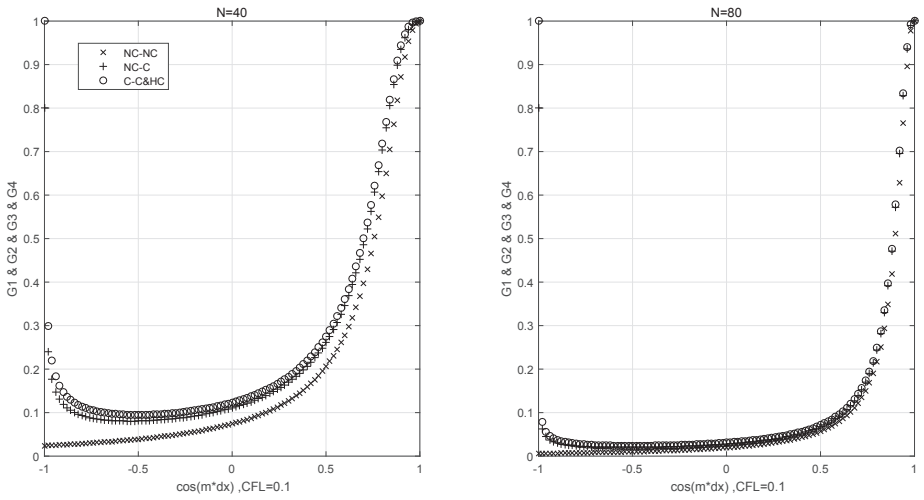

Figure 1: The amplification factors of P^0, Euler backward/forward scheme: For P^0 numerical approximation in linear case, C-C and HC schemes are equivalent.

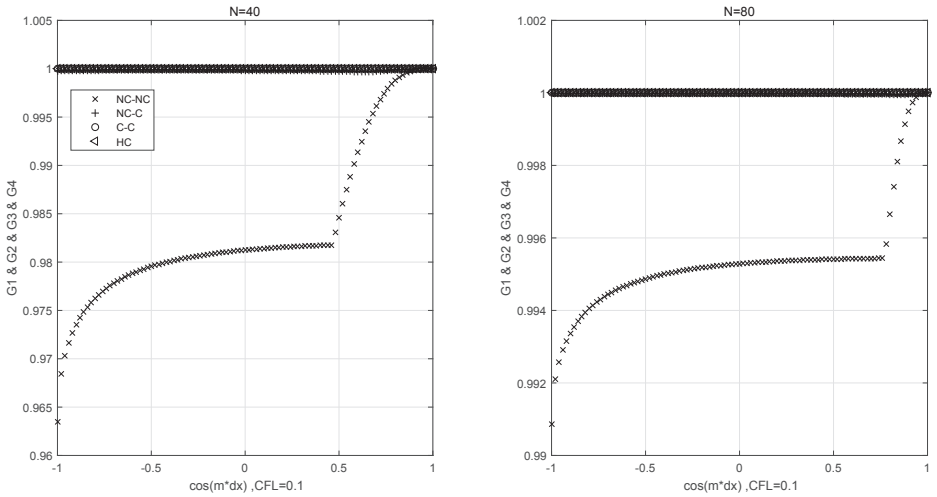

Figure 2: The amplification factors of P^1, second-order mid-point scheme.

experiments using C-NC scheme are identical to those of NC-NC scheme, therefore we do not list the C-NC scheme. This fact is part of the evidence supporting the opinion that conservative treatment for the dispersive term F_I has a much larger effect on the result than using the conservative scheme for F_E.

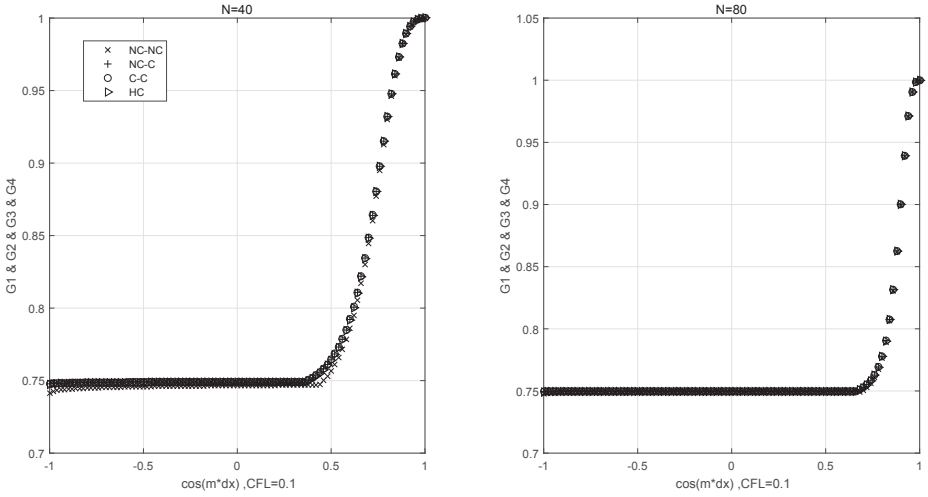

Figure 3: The amplification factors of P^1, second-order SDC scheme (SDC2).

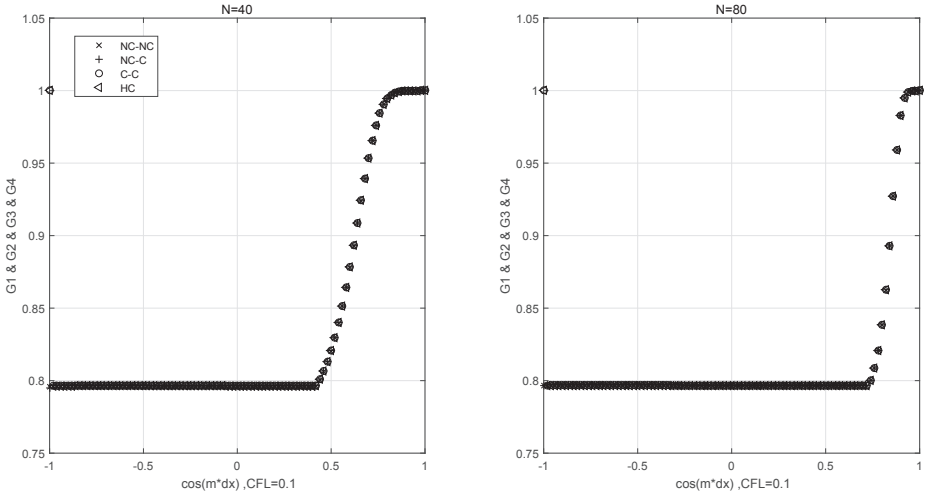

Figure 4: The amplification factors of P^2, third-order SDC scheme (SDC3).

Example 4.1. We first consider linear KdV equation

$$u_t+u_x+u_{xxx}=0. \tag{4.1}$$

We use two initial conditions to compare order of accuracy, and we can see how the order of accuracy acts on different frequency. The first is

$$u(x,0)=\sin\left(\frac{1}{2}x\right), \tag{4.2}$$

Table 2: Single wave case of linear KdV in Example 4.1 at $T=1$.

	N	$\|e\|_{L^2}$	order	$\|e\|_\infty$	order	$\|e\|_{L^2}$	order	$\|e\|_\infty$	order	$\|e\|_{L^2}$	order	$\|e\|_\infty$	order
		P^2, SDC3				P^2, mid-point				P^3, SDC4			
NC-NC	20	6.22E-05	–	3.06E-04	–	4.90E-05	–	2.00E-04	–	2.19E-06	–	8.97E-06	–
	40	7.76E-06	3.00	3.84E-05	2.99	6.14E-06	3.00	2.47E-05	3.02	1.38E-07	3.99	5.63E-07	3.99
	80	9.70E-07	3.00	4.79E-06	3.00	1.03E-06	2.58	5.06E-06	2.29	8.60E-09	4.00	3.52E-08	4.00
	160	1.21E-07	3.00	5.99E-07	3.00	1.21E-07	3.09	5.96E-07	3.08	5.38E-10	4.00	2.20E-09	4.00
	320	1.52E-08	3.00	7.49E-08	3.00	1.52E-08	3.00	7.48E-08	2.99	3.36E-11	4.00	1.38E-10	4.00
NC-C	20	6.25E-05	–	3.07E-04	–	7.50E-05	–	3.15E-04	–	2.12E-06	–	7.98E-06	–
	40	7.77E-06	3.01	3.84E-05	3.00	1.24E-05	2.59	5.17E-05	2.61	1.33E-07	3.99	5.01E-07	3.99
	80	9.70E-07	3.00	4.80E-06	3.00	2.05E-06	2.60	1.18E-05	2.13	8.34E-09	4.00	3.14E-08	4.00
	160	1.21E-07	3.00	5.99E-07	3.00	2.87E-07	2.84	1.58E-06	2.90	5.21E-10	4.00	1.96E-09	4.00
	320	1.52E-08	3.00	7.49E-08	3.00	2.21E-08	3.70	1.17E-07	3.75	3.26E-11	4.00	1.23E-10	4.00
C-C	20	6.25E-05	–	3.07E-04	–	7.57E-05	–	3.18E-04	–	2.12E-06	–	7.98E-06	–
	40	7.77E-06	3.01	3.84E-05	3.00	1.25E-05	2.60	5.19E-05	2.62	1.33E-07	3.99	5.01E-07	3.99
	80	9.70E-07	3.00	4.80E-06	3.00	2.05E-06	2.61	1.18E-05	2.13	8.34E-09	4.00	3.14E-08	4.00
	160	1.21E-07	3.00	5.99E-07	3.00	2.87E-07	2.84	1.58E-06	2.91	5.21E-10	4.00	1.96E-09	4.00
	320	1.52E-08	3.00	7.49E-08	3.00	2.21E-08	3.70	1.18E-07	3.75	3.26E-11	4.00	1.23E-10	4.00
HC	20	3.78E-05	–	1.92E-04	–	1.63E-04	–	5.96E-04	–	1.75E-06	–	7.84E-06	–
	40	4.67E-06	3.02	2.41E-05	2.99	1.66E-05	3.29	7.94E-05	2.91	1.10E-07	4.00	4.93E-07	3.99
	80	5.82E-07	3.00	3.02E-06	3.00	1.81E-06	3.19	8.21E-06	3.27	6.85E-09	4.00	3.08E-08	4.00
	160	7.27E-08	3.00	3.77E-07	3.00	2.78E-07	2.70	1.12E-06	2.88	4.28E-10	4.00	1.93E-09	4.00
	320	9.09E-09	3.00	4.72E-08	3.00	2.17E-08	3.68	1.23E-07	3.19	2.68E-11	4.00	1.20E-10	4.00

with the frequency (or wavenumber) $m=\frac{1}{2}$. The exact solution is given by

$$u(x,t)=\sin\Big(\frac{1}{2}x-\frac{3}{8}t\Big). \tag{4.3}$$

The other initial condition is

$$u(x,0)=e^{\sin x}, \tag{4.4}$$

which does not have an analytic solution. The exact solution of initial condition (4.4) can be written by Taylor expansion in a sum of sine functions with different frequency. Then we can see the influence of frequency of wave. For those two cases, we both take periodic boundary condition. The period L of initial condition (4.2) is 4π, that of initial condition (4.4) is 2π. The time step is taken as $\Delta t=\mathcal{O}(\Delta x)$.

The L^2 and L^∞ error, $\|u-u_h\|_{L^2}$ and $\|u-u_h\|_{L^\infty}$, and the convergence rate of the initial condition (4.2), (4.4) at $T=1$ are contained in Table 2 and Table 3, respectively. As distinct from the initial condition (4.2), we get that the convergence rate of multi-frequency wave is slower than that of single wave. However, both cases can reach the optimal convergence error order $(k+1)$-th in both norms. The exact solution of initial condition (4.4) can be considered as a series of multi-frequency wave, while the exact solution (4.3) is just one sine function with a single frequency. It means that the multi-frequency wave has more complex structure than the single frequency wave. Owning to the stability analysis, we can see that the change of frequency have some effects on the numerical results.

Table 3: Multi-frequency wave case of linear KdV in Example 4.1 at $T=1$.

	N	$\|e\|_{L^2}$	order	$\|e\|_\infty$	order	$\|e\|_{L^2}$	order	$\|e\|_\infty$	order
	P^k	P^2				P^3			
NC-NC	20	4.19E-03	–	1.90E-02	–	1.44E-03	–	4.91E-03	–
	40	1.41E-03	1.57	5.68E-03	1.74	2.76E-04	2.38	1.11E-03	2.15
	80	3.23E-04	2.13	1.54E-03	1.89	4.01E-05	2.78	1.78E-04	2.64
	160	5.71E-05	2.50	2.78E-04	2.47	3.62E-06	3.47	1.63E-05	3.45
	320	7.82E-06	2.87	3.33E-05	3.06	2.30E-07	3.97	8.14E-07	4.32
	640	9.74E-07	3.01	3.81E-06	3.13	1.38E-08	4.06	5.24E-08	3.96
NC-C	20	2.77E-03	–	1.71E-02	–	1.44E-03	–	4.95E-03	–
	40	1.38E-03	1.00	5.66E-03	1.59	2.76E-04	2.39	1.11E-03	2.15
	80	3.23E-04	2.10	1.54E-03	1.88	4.01E-05	2.78	1.78E-04	2.65
	160	5.71E-05	2.50	2.78E-04	2.46	3.62E-06	3.47	1.63E-05	3.45
	320	7.82E-06	2.87	3.33E-05	3.06	2.30E-07	3.97	8.14E-07	4.32
	640	9.74E-07	3.01	3.81E-06	3.13	1.38E-08	4.06	5.24E-08	3.96
C-C	20	2.77E-03	–	1.71E-02	–	1.44E-03	–	4.95E-03	–
	40	1.38E-03	1.00	5.66E-03	1.59	2.76E-04	2.39	1.11E-03	2.15
	80	3.23E-04	2.10	1.54E-03	1.88	4.01E-05	2.78	1.78E-04	2.65
	160	5.71E-05	2.50	2.78E-04	2.46	3.62E-06	3.47	1.63E-05	3.45
	320	7.82E-06	2.87	3.33E-05	3.06	2.30E-07	3.97	8.14E-07	4.32
	640	9.74E-07	3.01	3.81E-06	3.13	1.38E-08	4.06	5.24E-08	3.96
HC	20	2.77E-03	–	1.67E-02	–	1.44E-03	–	4.82E-03	–
	40	1.38E-03	1.01	6.07E-03	1.46	2.76E-04	2.38	1.15E-03	2.06
	80	3.23E-04	2.10	1.58E-03	1.94	4.01E-05	2.79	1.77E-04	2.70
	160	5.71E-05	2.50	2.83E-04	2.48	3.62E-06	3.47	1.63E-05	3.44
	320	7.82E-06	2.87	3.32E-05	3.09	2.30E-07	3.97	8.13E-07	4.32
	640	9.73E-07	3.01	3.80E-06	3.13	1.38E-08	4.06	5.24E-08	3.96

Thus, the energy of numerical scheme for multi-frequency wave is slightly ascending as wave propagates, see Fig. 7.

We compare the semi-implicit SDC time discretization scheme with the mid-point time discretization scheme. In Table 2, Fig. 5, since the semi-implicit SDC scheme is non-conservative, then all four schemes influenced by time discretization have similar numerical results. When we take mid-point scheme as time discretization scheme, we can see the differences of four kinds of spatial discretization schemes, for C-C scheme, the energy is a invariant up to round-off error, see the right graph of Fig. 5. Although another three schemes have some dissipation, the energy changes slightly. We also plot the error of Hamiltonian H_2 in Fig. 6 for the third and fourth order schemes. Similarly, high order schemes can reduce the fluctuation in Hamiltonian effectively.

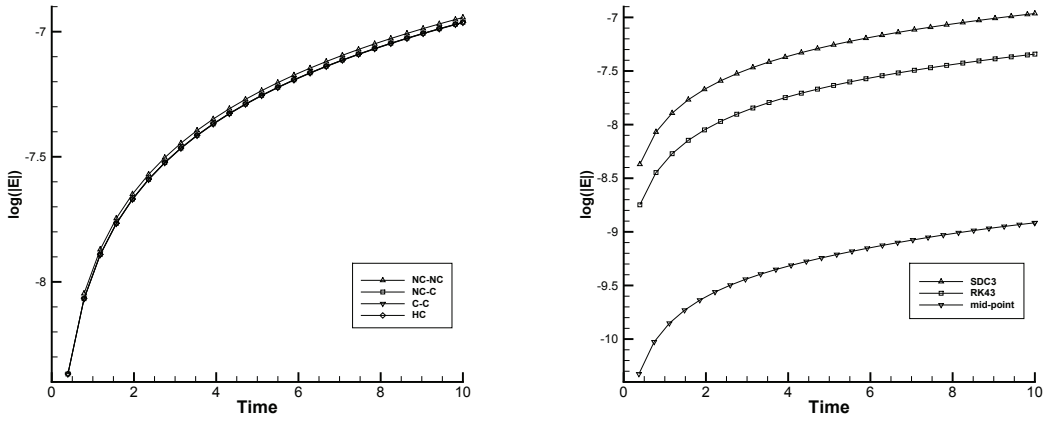

Figure 5: The error of L^2 energy ($E=H_1(t)-H_1(0)$) of single wave case for linear KdV (4.1): NC-NC, NC-C, C-C, HC scheme with SDC3 on the left; C-C scheme with SDC3, RK43 (four stage, third order), mid-point time scheme on the right; comparison when $k=2$.

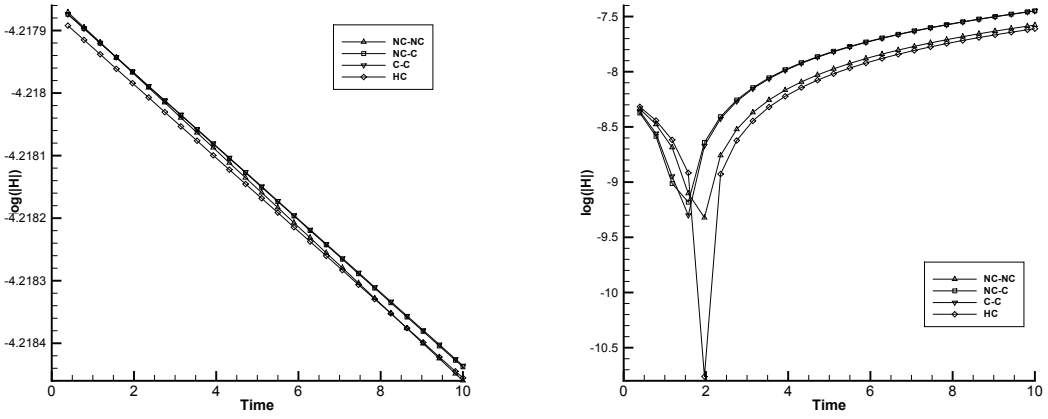

Figure 6: The error of Hamiltonian ($H=H_2(t)-H_2(0)$) of NC-NC, NC-C, C-C and HC schemes for single wave case of linear KdV (4.1): $k=2$, SDC3 on the left; $k=3$, SDC4 on the right.

Owing to the semi-implicit SDC time discretization, we can choose time step $\Delta t = O(\Delta x)$, CFL number 0.1, even a larger CFL condition number. From Tables 2 and 3, NC-NC, NC-C, C-C, HC these four kinds of spatial discretization schemes have similar numerical accuracy. In addition, the dissipative NC-NC scheme also has a good accuracy in Table 2 as well as conservative schemes i.e. C-C and HC schemes. But for long temporal interval $T=500$, dissipation will cause phase error which can be reduced by high order numerical approximation, see Fig. 9.

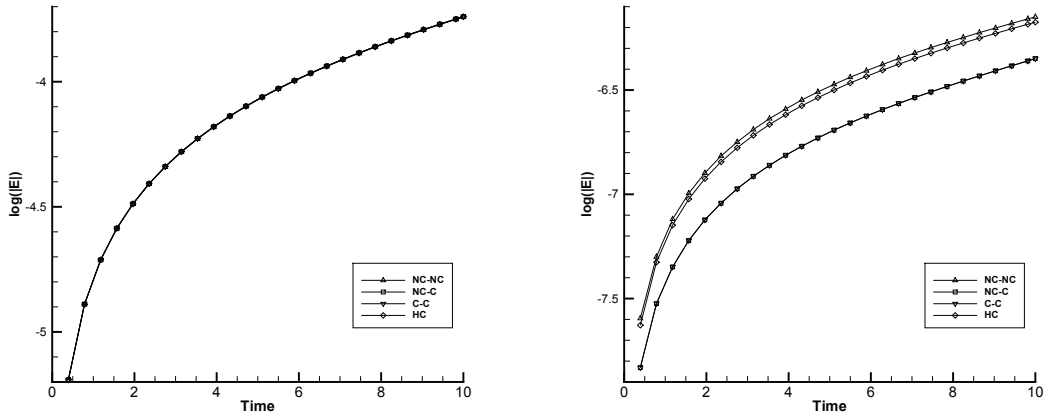

Figure 7: The error of L^2 energy ($E=H_1(t)-H_1(0)$) of NC-NC, NC-C, C-C and HC schemes for multi-frequency wave case of linear KdV (4.1): $k=2$, SDC3 on the left; $k=3$, SDC4 on the right.

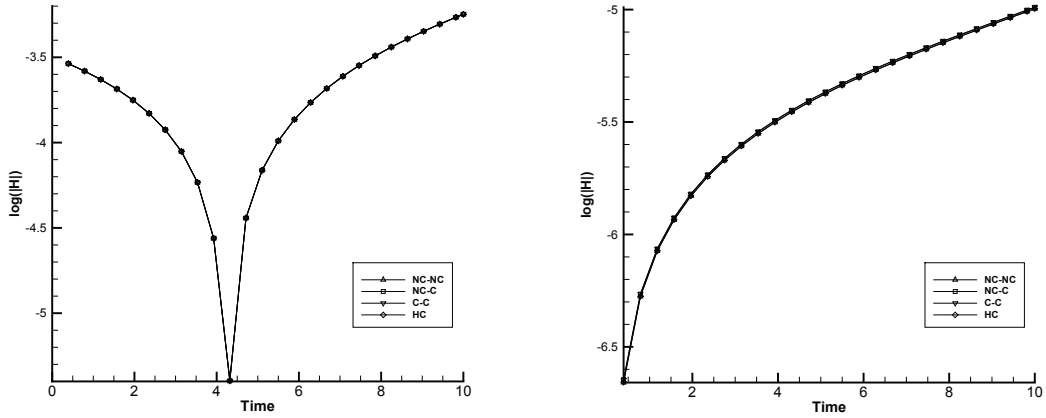

Figure 8: The error of Hamiltonian ($H=H_2(t)-H_2(0)$) of NC-NC, NC-C, C-C and HC schemes for multi-frequency wave case of linear KdV (4.1): $k=2$, SDC3 on the left; $k=3$, SDC4 on the right.

For initial condition (4.4), L^2 energy H_1 of all four schemes is slightly ascending in Fig. 7 resulting from the multi-frequency of wave. We can see that SDC4 schemes have less change in energy than SDC3 schemes in Fig. 7. In Fig. 8, we show the error of Hamiltonian for the third and fourth order schemes. It tells that adopting high order discretization methods can reduce the energy H_1 and Hamiltonian H_2 fluctuations effectively, even though the fully discrete schemes are no longer conservative in H_1 and H_2.

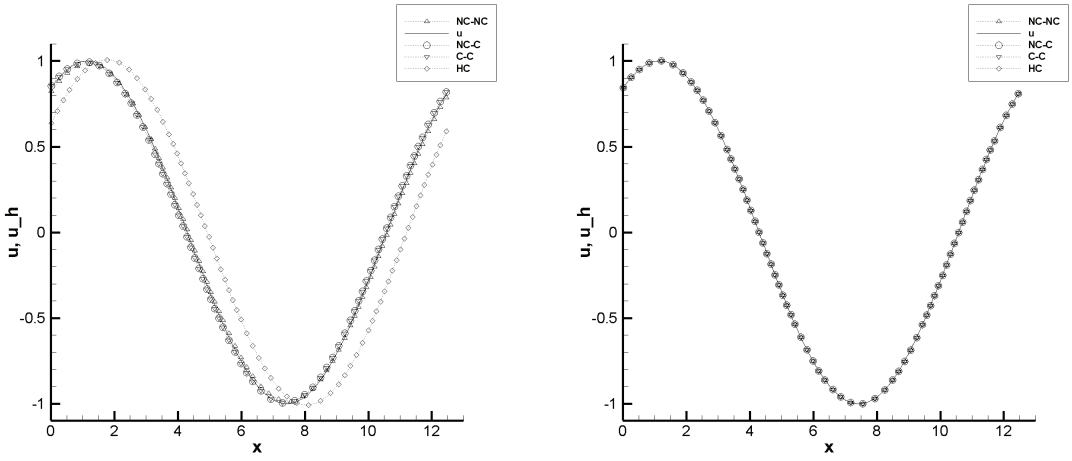

Figure 9: Single wave case of linear KdV (4.1): P^1, SDC2 on the left; P^2, SDC3 on the right; comparison with $N=40$ and time $T=500$.

Example 4.2. We show an accuracy test and energy variety for nonlinear KdV equation

$$u_t+(3u^2)_x+u_{xxx}=0 \tag{4.5}$$

with initial condition

$$u(x,0)=\frac{1}{2}\text{sech}^2\Big(\frac{1}{2}x\Big). \tag{4.6}$$

The exact solution is

$$u(x,t)=\frac{1}{2}\text{sech}^2\Big(\frac{1}{2}(x-t)\Big). \tag{4.7}$$

The computational domain is given by $[-50,50]$, and boundary condition is taken as periodic boundary, period $L=2\pi$. The time step is chosen as $\Delta t=O(\Delta x)$ with CFL number 0.1, In Table 4, we notice that these four numerical schemes expect C-C scheme can achieve the optimal accuracy order for nonlinear KdV equation (4.5). For C-C scheme, the order of error varies with parity of k somehow. For even k, we can get the optimal accuracy order $(k+1)$-*th*, however, for odd k, we can only get suboptimal accuracy. The L^2 conservative scheme with numerical fluxes (2.24) in [16] and the Hamiltonian conservative scheme in [18] have the similar order reduction.

In Fig. 10, we plot the L^2 energy graph of SDC2 time discretization on the left and the C-C cases combined with different time discretization schemes are listed on the right. The energy fluctuation of second-order numerical scheme is larger than that of higher order numerical scheme in Fig. 11. As shown in Fig. 11, if we upgrade the order of time and space discretization, the dissipation will be decreased. The high order dissipative numerical scheme have little difference with conservative numerical scheme on energy

Table 4: Nonlinear KdV in Example 4.2 at $T=1$.

	N	$\|e\|_{L^2}$	order	$\|e\|_\infty$	order	$\|e\|_{L^2}$	order	$\|e\|_\infty$	order
		P^2				P^3			
NC-NC	40	1.69E-03	–	2.12E-02	–	5.43E-04	–	8.33E-03	–
	80	2.19E-04	2.94	4.30E-03	2.30	2.88E-05	4.24	4.19E-04	4.31
	160	2.51E-05	3.13	5.82E-04	2.88	2.13E-06	3.75	3.96E-05	3.40
	320	3.15E-06	2.99	7.63E-05	2.93	1.39E-07	3.94	2.48E-06	4.00
	640	3.95E-07	3.00	9.67E-06	2.98	8.77E-09	3.99	1.58E-07	3.98
NC-C	40	4.06E-03	–	3.63E-02	–	5.80E-04	–	7.83E-03	–
	80	3.06E-04	3.73	7.78E-03	2.22	2.88E-05	4.33	4.63E-04	4.08
	160	2.60E-05	3.56	6.31E-04	3.62	2.06E-06	3.80	3.44E-05	3.75
	320	3.18E-06	3.03	7.82E-05	3.01	1.34E-07	3.94	2.02E-06	4.09
	640	3.96E-07	3.01	9.76E-06	3.00	8.49E-09	3.99	1.29E-07	3.98
C-C	40	5.23E-03	–	3.80E-02	–	1.12E-03	–	8.91E-03	–
	80	9.48E-04	2.47	1.07E-02	1.82	3.16E-05	5.15	4.76E-04	4.23
	160	2.63E-05	5.17	6.31E-04	4.09	2.61E-06	3.60	3.95E-05	3.59
	320	3.19E-06	3.04	7.84E-05	3.01	2.44E-07	3.41	2.72E-06	3.86
	640	3.96E-07	3.01	9.76E-06	3.01	2.70E-08	3.18	2.18E-07	3.64
HC	40	6.56E-03	–	5.03E-02	–	6.15E-04	–	9.50E-03	–
	80	2.30E-04	4.83	3.52E-03	3.84	2.69E-05	4.51	3.47E-04	4.77
	160	1.58E-05	3.86	3.54E-04	3.31	1.94E-06	3.79	3.06E-05	3.51
	320	1.91E-06	3.05	4.82E-05	2.88	1.27E-07	3.94	1.89E-06	4.01
	640	2.38E-07	3.01	6.13E-06	2.97	7.99E-09	3.99	1.22E-07	3.96

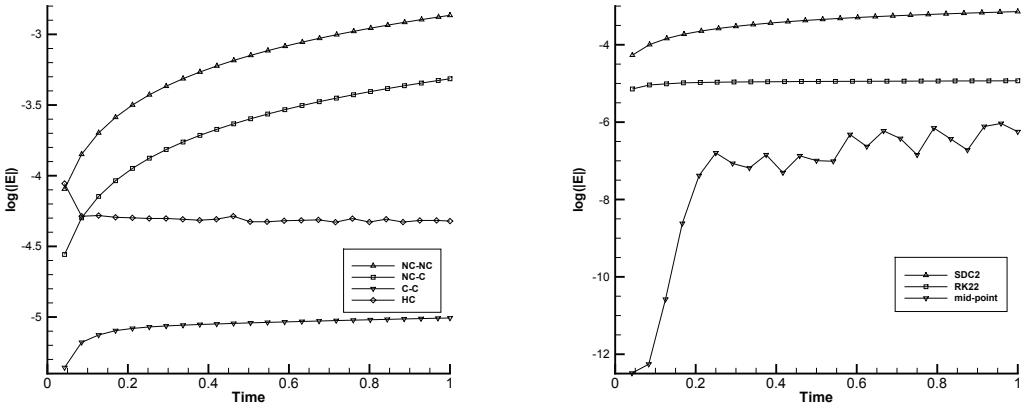

Figure 10: The error of L^2 energy ($E=H_1(t)-H_1(0)$) for nonlinear KdV (4.5): NC-NC, NC-C, C-C and HC schemes with SDC2 on the left; C-C scheme with SDC2, RK22(two stage, second order), and mid-point time schemes on the right; comparison when $k=1$.

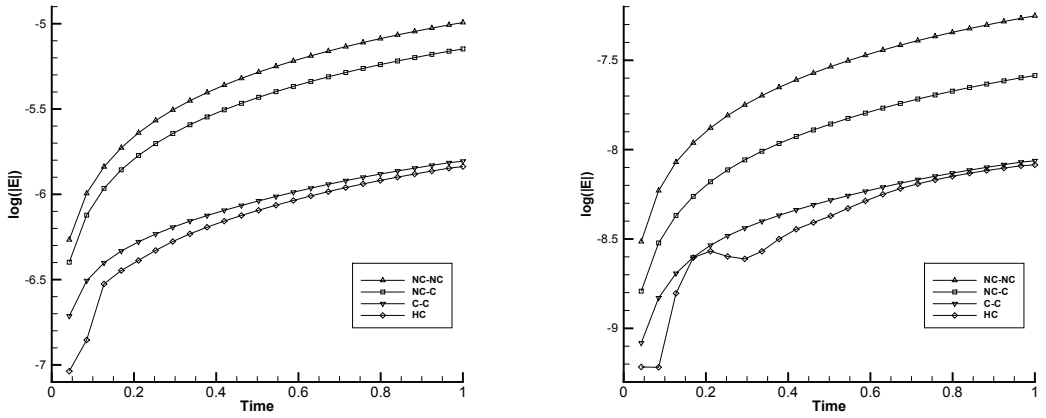

Figure 11: The error of L^2 energy($E=H_1(t)-H_1(0)$) of NC-NC, NC-C, C-C and HC schemes for nonlinear KdV (4.5): $k=2$, SDC3 on the left; $k=3$, SDC4 on the right.

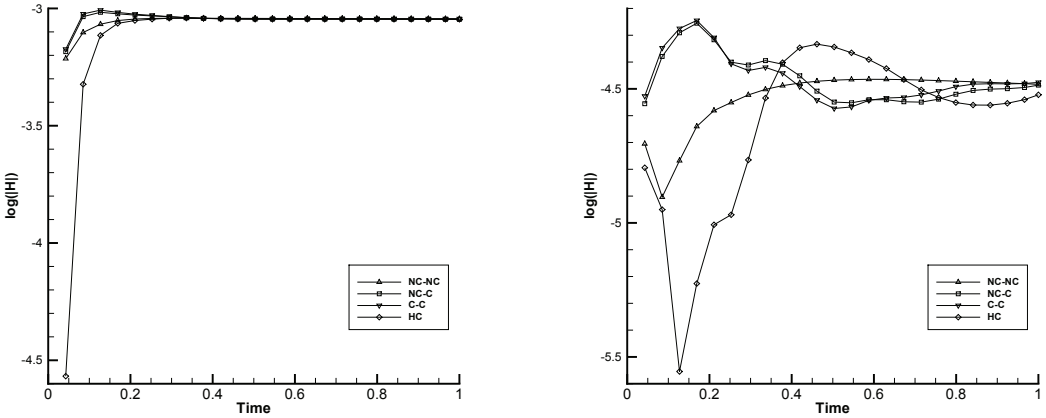

Figure 12: The error of Hamiltonian ($H=H_2(t)-H_2(0)$) of NC-NC, NC-C, C-C and HC schemes for nonlinear KdV (4.5): $k=2$, SDC3 on the left; $k=3$, SDC4 on the right.

variety. In Table 5, we list the differences of energy of two schemes from $t=0$ to $t=1$, respectively. i.e.

$$\Delta E=\sum_j\Big(\int_{I_j}u_h^2\Big|_{t=1}\,dx-\int_{I_j}u_0^2\,dx\Big). \tag{4.8}$$

We notice high order scheme can reduce the dissipation of energy effectively. For same accuracy order, the dissipation of C-C and HC scheme are smaller than the other two schemes. We conclude that high order accuracy numerical scheme and conservativeness can help to reduce the dissipation of energy. Also in Fig. 12 and Table 6, the error of

Table 5: Energy change of two schemes for nonlinear KdV (4.5): SDC3, P^2 and SDC4, P^3.

$\|\Delta E\|$	SDC3 P^2	SDC4 P^3
NC-NC	1.02E-05	5.61E-08
NC-C	7.11E-06	2.60E-08
C-C	1.56E-06	8.66E-09
HC	1.45E-06	8.22E-09

Table 6: H_2 change of two schemes for nonlinear KdV (4.5): SDC3, P^2 and SDC4, P^3.

$\|\Delta H\|$	SDC3 P^2	SDC4 P^3
NC-NC	9.02E-04	3.29E-05
NC-C	8.98E-04	3.27E-05
C-C	9.04E-04	3.34E-05
HC	8.99E-04	3.01E-05

Hamiltonian H_2 evolution is plotted for the third and fourth order schemes. It shows that high order schemes can also reduce the error in Hamiltonian effectively, even though the fully discrete schemes are not conservative in Hamiltonian.

Example 4.3. We give another nonlinear KdV equation by setting $\varepsilon = 1/24^2$

$$u_t + \frac{1}{2}(u^2)_x + \varepsilon u_{xxx} = 0. \tag{4.9}$$

The computational domain was set to $[0,1]$, we use two well-known solutions of (4.9) to check accuracy and convergence rate. The first one is called cnoidal-wave solution,

$$u(x,t) = acn^2(4K(x - vt - x_0)), \tag{4.10}$$

where

$$\begin{aligned} a &= 192m\varepsilon K(m)^2, \\ v &= 64\varepsilon(2m-1)K(m)^2. \end{aligned} \tag{4.11}$$

The function $cn(z) = cn(z:m)$ is the Jacobi elliptic function with modulus $m \in (0,1)$, see [1]. In this numerical experiment we take $m = 0.9$, and $K = K(m)$ is the complete elliptic integral of the first kind. The parameter x_0 is arbitrary, we take it as zero. The solution u has spatial period 1.

First we take the degree of discontinuous finite element space $k = 2$. From Table 7, we can see that the errors of NC-NC, NC-C schemes between numerical solutions and exact solution are a bit large at $T = 10$ when the number of cells N equals 20. In order to figure out the reason, we plot the Fig. 13(a). The NC-NC and NC-C schemes have phase

Table 7: Cnoidal wave case for nonlinear KdV in Example 4.3: P^2, SDC3.

	N	$\|e\|_{L^2}$	order	$\|e\|_\infty$	order	$\|e\|_{L^2}$	order	$\|e\|_\infty$	order
	T	$T=1.0$				$T=10.0$			
NC-NC	20	3.66E-03	4.21	1.72E-02	3.92	0.25	–	0.84	–
	40	2.07E-04	4.14	1.20E-03	3.85	1.14E-02	4.46	3.91E-02	4.43
	80	2.19E-05	3.24	1.56E-04	2.94	5.49E-04	4.38	1.96E-03	4.32
	160	2.71E-06	3.02	2.04E-05	2.94	4.02E-05	3.77	1.47E-04	3.73
	320	3.38E-07	3.00	2.57E-06	2.99	4.10E-06	3.29	1.53E-05	3.27
NC-C	20	3.39E-03	4.50	1.74E-02	4.03	2.59E-01	–	8.70E-01	–
	40	1.85E-04	4.19	1.16E-03	3.90	7.46E-03	5.12	2.58E-02	5.08
	80	2.18E-05	3.09	1.60E-04	2.86	4.14E-04	4.17	1.49E-03	4.11
	160	2.71E-06	3.01	2.05E-05	2.96	3.58E-05	3.53	1.32E-04	3.50
	320	3.38E-07	3.00	2.58E-06	2.99	3.62E-06	3.31	1.36E-05	3.28
C-C	20	2.93E-03	2.63	1.69E-02	2.05	5.26E-03	–	2.57E-02	–
	40	1.75E-04	4.07	1.32E-03	3.68	1.85E-03	1.51	6.88E-03	1.90
	80	2.17E-05	3.01	1.63E-04	3.02	2.42E-04	2.93	9.06E-04	2.92
	160	2.70E-06	3.00	2.06E-05	2.99	3.05E-05	2.99	1.14E-04	2.99
	320	3.38E-07	3.00	2.59E-06	2.99	3.45E-06	3.14	1.31E-05	3.13
HC	20	9.64E-04	3.74	5.38E-03	3.54	1.79E-02	–	6.31E-02	–
	40	1.04E-04	3.22	7.60E-04	2.83	1.93E-03	3.21	6.80E-03	3.21
	80	1.29E-05	3.01	1.01E-04	2.90	2.43E-04	2.99	8.72E-04	2.96
	160	1.61E-06	3.00	1.28E-05	2.98	3.05E-05	2.99	1.10E-04	2.99
	320	2.02E-07	3.00	1.60E-06	3.01	4.27E-06	2.84	1.53E-05	2.84

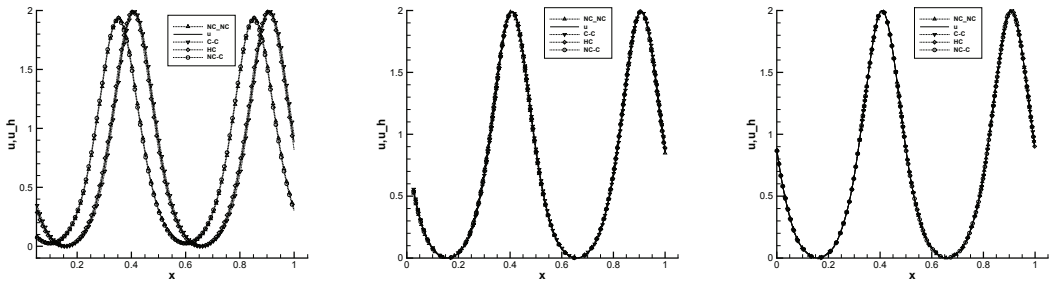

(a) $N=20$ (b) $N=40$ (c) $N=80$

Figure 13: Cnoidal wave case for nonlinear KdV (4.9): numerical approximations of NC-NC, NC-C, C-C, HC scheme with SDC3 time discretization, comparison at $k=2$ and $T=10$.

error and a little decay in amplitude which makes the numerical solution inaccurate. In contrast with above two schemes, the C-C and HC schemes demonstrate a better behavior in numerical approximation. The dissipation is the main reason for phase error and

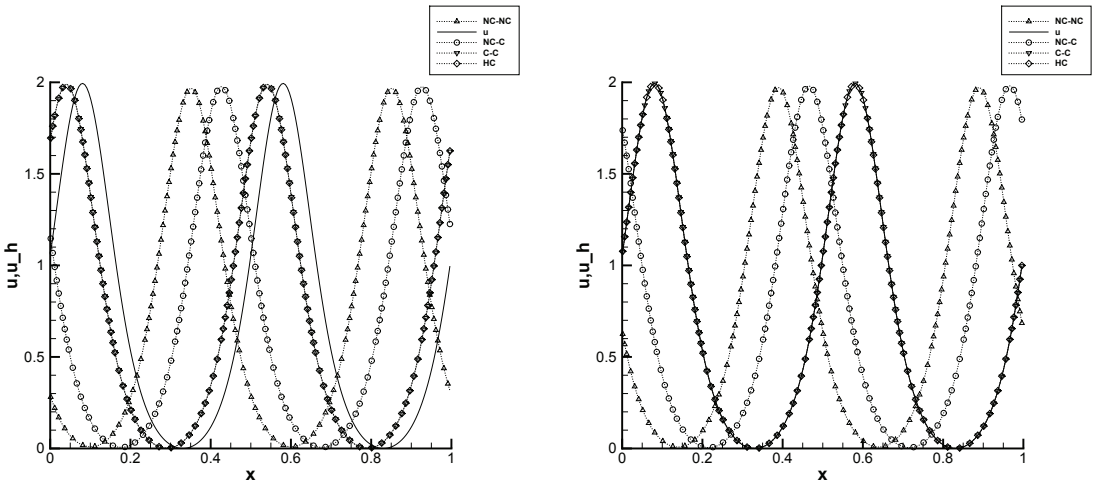

(a) $N=40$ (b) $N=40$

Figure 14: NC-NC, NC-C, C-C and HC schemes of cnoidal wave case for nonlinear KdV (4.9): SDC3 time discretization on the left; SDC4 time discretization on the right, comparison at $k=2$ and $T=100$.

amplitude decay, it slows the propagation of wave and decay the energy. Nevertheless, the phase error and amplitude decay will vanish when we refine the spatial partition in Fig. 13(b),(c). We know that the propagation of wave decays as time increases, so we also list long time results which $T=100$. In the left graph of Fig. 14, the effect of dissipation causes varying degrees of phase error for all four kinds of schemes. The L^2 conservative scheme combined with conservative time discretization in [16] does not have visible phase error in the experiments. From the left graph to right graph of Fig. 14, we improve the order of time discretization and the phase error minish obviously, especially for C-C and HC scheme.

Next, we improve the spatial discretization with $k=4$. To compare with P^2, SDC3 case, we still use SDC3 as time discretization scheme in the left graph of Fig. 15, so that we can see the effect of spatial discretization. For all four kinds of spatial discretization schemes, the phase error reduces to a large extent but it still has visible errors. When we upgrade both time and space accuracy orders, even for dissipative spatial discretization, a good accuracy can be obtained in the right graph of Fig. 15. We conclude that high order time discretization scheme can reduce the phase error validly for conservative spatial discretization scheme. For dissipative spatial discretization scheme, we need upgrade the accuracy order of time and space discretization both to obtain a good resolution of the numerical solution.

The another solution is solitary-wave solution

$$u(x,t)=A\text{sech}^2(K(x-vt-x_0)), \tag{4.12}$$

where $A=1$, $v=A/3$, $K=\frac{1}{2}\sqrt{\frac{A}{3\varepsilon}}$ and $x_0=\frac{1}{2}$, the wave commences its evolution centered in

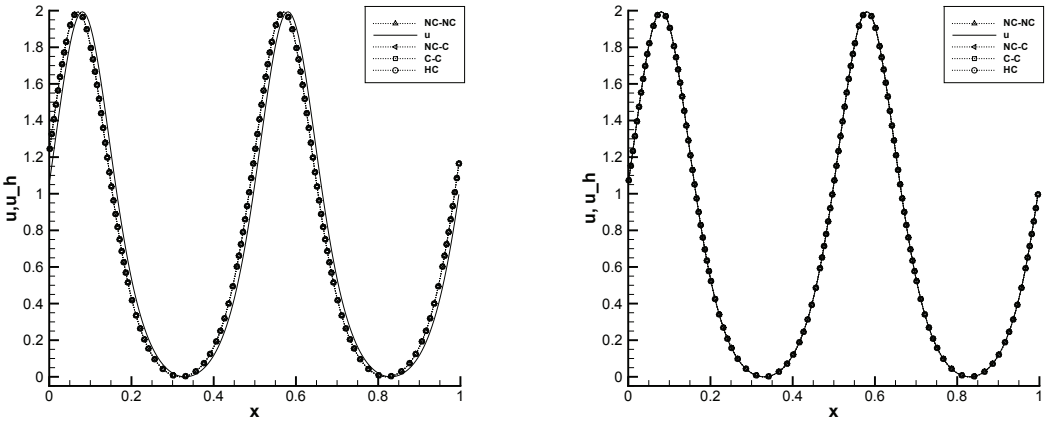

(a) $N=40$ (b) $N=40$

Figure 15: NC-NC, NC-C, C-C and HC schemes of cnoidal wave case for nonlinear KdV (4.9): P^4, SDC3 time discretization on the left; P^4, SDC4 time discretization on the right, comparison at $T=100$.

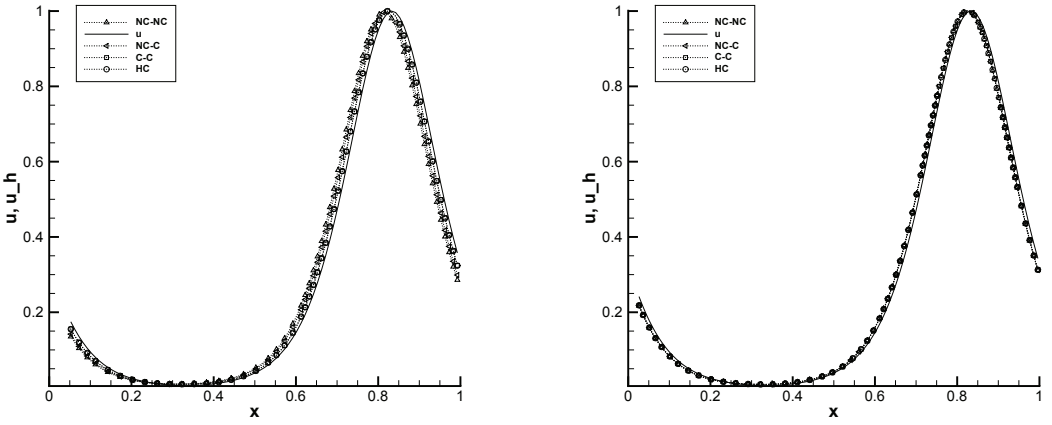

(a) $N=20$ (b) $N=40$

Figure 16: Solitary wave case for nonlinear KdV (4.9): numerical approximations of NC-NC, NC-C, C-C and HC schemes; comparison at $k=2$ and $T=25$.

the period domain. Because of the exponential decay of the solution, we can treat as a periodic problem in the domain $[0,1]$. This solitary wave solution is consistent with cnoidal wave, so we present only a small part of result of solitary wave in Fig. 16. Again, the phase error can be observed at $k=2$ and time $T=25$. And high order time discretization scheme can reduce it validly.

It is notable that we take $\theta_1=0.0$, $\theta_2=\frac{2}{3}$ in Example 4.3 for all SDC schemes to avoid instability.

Example 4.4. In this example, we show numerical approximation of soliton solution for the KdV type equation

$$u_t+\frac{1}{2}(u^2)_x+u_{xxx}=0. \tag{4.13}$$

We list a 2-soliton solution derived from [6].

$$u(x,t)=12\frac{\kappa_1^2e^{\theta_1}+\kappa_2^2e^{\theta_2}+2(\kappa_2-\kappa_1)^2e^{\theta_1+\theta_2}+a^2(\kappa_2^2e^{\theta_1}+\kappa_1^2e^{\theta_2})e^{\theta_1+\theta_2}}{(1+e^{\theta_1}+e^{\theta_2}+a^2e^{\theta_1+\theta_2})^2}, \tag{4.14}$$

where

$$\begin{aligned}&\kappa_1=0.4,\quad \kappa_2=0.6,\quad a^2=\left(\frac{\kappa_1-\kappa_2}{\kappa_1+\kappa_2}\right)^2,\\&\theta_1=\kappa_1x-\kappa_1^3t+4,\quad \theta_2=\kappa_2x-\kappa_2^3t+15.\end{aligned} \tag{4.15}$$

The computational domain is set to $[-40,40]$ with periodic boundary condition. To demonstrate the effectiveness of the high order schemes, we test all four schemes with P^2 approximation space and SDC3 time discretization and $N=160$, $\Delta t=0.1\Delta x$. The numerical results of four schemes are listed in Fig. 17. There is no visible phase error and shape error between all numerical solutions and exact solution.

5 Conclusion

In this paper, we proposed L^2 conservative and Hamiltonian conservative LDG numerical schemes with the minimal stencil. Compared with the dissipative LDG numerical scheme, the conservative LDG numerical scheme for the Korteweg-de Vries type equation can help to reduce the phase error in the propagation of wave effectively, especially in low order approximation. For linear KdV equations, all four spatial discretization schemes NC-NC, NC-C, C-C and HC can achieve optimal order of convergence rate numerically. However, for nonlinear KdV equations, C-C scheme obtains only suboptimal accuracy order for odd degree polynomial space numerically. Meanwhile, the HC scheme we constructed maintains optimal accuracy order for both even and odd degree polynomial space in our numerical experiments. We also adopt the high order semi-implicit SDC scheme for temporal discretization. It is found that high order numerical schemes can reduce the dissipation validly as well as conservative schemes.

Acknowledgments

The research of Y. Xia was partially supported by National Science Foundation of China grants No. 11471306 and No. 11871449, and a grant from the Science & Technology on Reliability & Environmental Engineering Laboratory (No. 6142A0502020817).

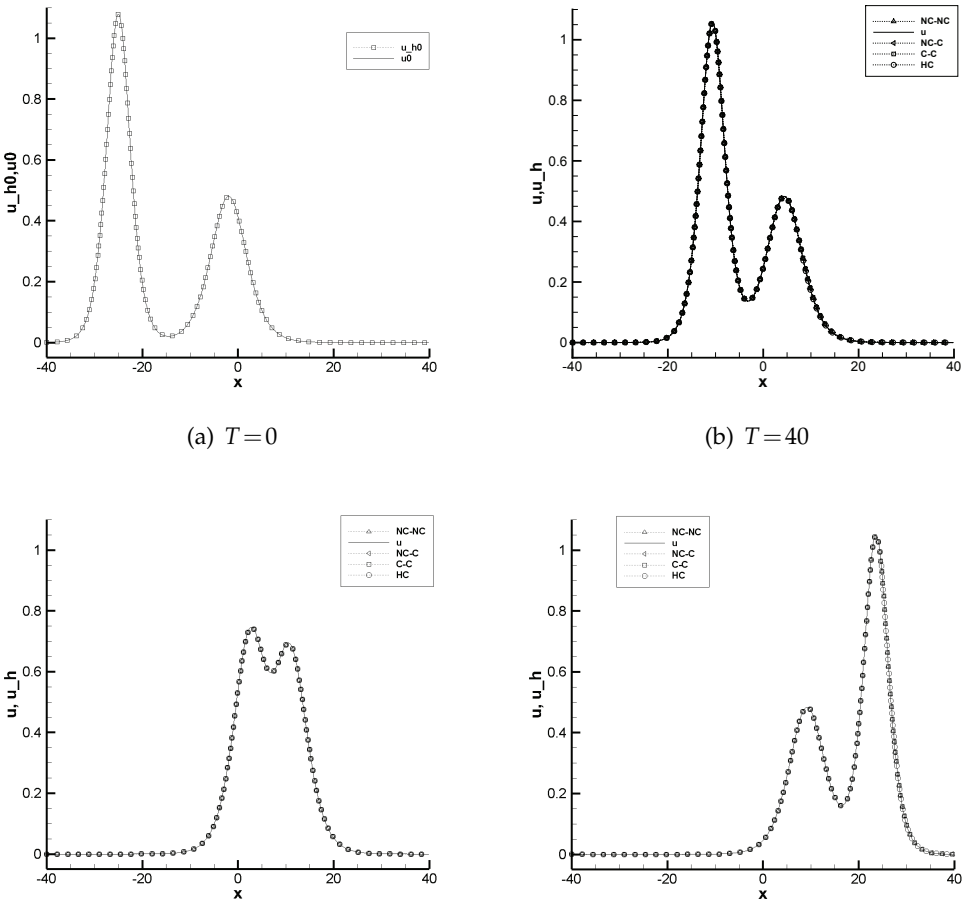

(a) $T=0$ (b) $T=40$

(c) $T=80$ (d) $T=120$

Figure 17: 2-soliton solution of nonlinear KdV (4.13): P^2, SDC3, $N=160$.

References

[1] M. Abramowitz and I.A. Stegun. Handbook of mathematical functions: with formulas, graphs, and mathematical tables. Vol. 55. Courier Corporation, 1964.

[2] U.M. Ascher, S.J. Ruuth and R.J. Spiteri. Implicit-explicit Runge-Kutta methods for time-dependent partial differential equations. Applied Numerical Mathematics, 1997, 25(2-3): 151-167.

[3] F. Bassi and S. Rebay. A high-order accurate discontinuous finite element method for the numerical solution of the compressible Navier-Stokes equations. Journal of Computational Physics, 1997, 131(2): 267-279.

[4] J. Bona, H. Chen, O. Karakashian and Y. Xing. Conservative, discontinuous Galerkin methods for the generalized Korteweg-de Vries equation. Mathematics of Computation, 2013,

82(283): 1401-1432.
[5] B. Cockburn and C.W. Shu. The local discontinuous Galerkin method for time-dependent convection-diffusion systems. SIAM Journal on Numerical Analysis, 1998, 35(6): 2440-2463.
[6] Y. Cui and D. Mao. Numerical method satisfying the first two conservation laws for the Korteweg-de Vries equation. Journal of Computational Physics, 2007, 227(1): 376-399.
[7] Y. Cheng and C.W. Shu. A discontinuous Galerkin finite element method for time dependent partial differential equations with higher order derivatives. Mathematics of Computation, 2008, 77(262): 699-730.
[8] K. Dekker and J.G. Verwer. Stability of Runge-Kutta methods for stiff nonlinear differential equations. Amsterdam-New York, North-Holland 1984.
[9] A. Dutt, L. Greengard and V. Rokhlin. Spectral deferred correction methods for ordinary differential equations. BIT Numerical Mathematics, 2000, 40(2): 241-266.
[10] B. Fornberg and G.B. Whitham. A numerical and theoretical study of certain nonlinear wave phenomena. Philosophical Transactions of the Royal Society of London A: Mathematical, Physical and Engineering Sciences, 1978, 289(1361): 373-404.
[11] C.S. Gardner. Korteweg-de Vries equation and generalizations. IV. The Korteweg-de Vries equation as a Hamiltonian system. Journal of Mathematical Physics, 1971, 12(8): 1548-1551.
[12] K. Goda. On stability of some finite difference schemes for the Korteweg-de Vries equation. Journal of the Physical Society of Japan, 1975, 39(1): 229-236.
[13] J. Guzmán and B. Rivière. Sub-optimal convergence of non-symmetric discontinuous Galerkin methods for odd polynomial approximations. Journal of Scientific Computing, 2009, 40(1): 273-280.
[14] D.J. Korteweg and G. de Vries. On the change of form of long waves advancing in a rectangular canal, and on a new type of long stationary waves. Philosophical Magazine, 1895, 39(5): 422-443.
[15] S. Kutluay, A.R. Bahadir and A. Özdeş. A small time solutions for the Korteweg-de Vries equation. Applied Mathematics and Computation, 2000, 107(2): 203-210.
[16] O. Karakashian and Y.L. Xing. A posteriori error estimates for conservative local discontinuous Galerkin methods for the generalized Korteweg-de Vries equation. Communications in Computational Physics, 2016, 20(01): 250-278.
[17] D. Levy, C.W. Shu and J. Yan. Local discontinuous Galerkin methods for nonlinear dispersive equations. Journal of Computational Physics, 2004, 196(2): 751-772.
[18] H. Liu and N. Yi. A Hamiltonian preserving discontinuous Galerkin method for the generalized Korteweg-de Vries equation. Journal of Computational Physics, 2016, 321: 776-796.
[19] W.H. Reed and T.R. Hill. Triangular mesh methods for the neutron transport equation. Los Alamos Report LA-UR-73-479, 1973.
[20] A.C. Vliegenthart. On finite-difference methods for the Korteweg-de Vries equation. Journal of Engineering Mathematics, 1971, 5(2): 137-155.
[21] Y. Xia, Y. Xu and C.W. Shu. Efficient time discretization for local discontinuous Galerkin methods. Discrete and Continuous Dynamical Systems Series B, 2007, 8(3): 677.
[22] Y. Xia, Y. Xu and C.W. Shu, Local discontinuous Galerkin methods for the generalized Zakharov system, Journal of Computational Physics, 2010, 229(4): 1238-1259.
[23] Y. Xia and Y. Xu. A conservative local discontinuous Galerkin method for the Schrödinger-KdV system, Communications in Computional Physics, 2014, 15(4): 1091-1107.
[24] Y. Xu and C.W. Shu. Local discontinuous Galerkin methods for three classes of nonlinear wave equations. Journal of Computational Mathematics, 2004: 250-274.
[25] Y. Xu and C.W. Shu. Local discontinuous Galerkin methods for nonlinear Schrödinger equa-

tions. Journal of Computational Physics, 2005, 205(1): 72-97.
[26] Y. Xu and C.W. Shu. Local discontinuous Galerkin methods for two classes of two-dimensional nonlinear wave equations. Physica D: Nonlinear Phenomena, 2005, 208(1): 21-58.
[27] Y. Xu and C.W. Shu. Local discontinuous Galerkin methods for the Kuramoto-Sivashinsky equations and the Ito-type coupled KdV equations. Computer Methods in Applied Mechanics and Engineering, 2006, 195(25): 3430-3447.
[28] Y. Xu and C.W. Shu. Error estimates of the semi-discrete local discontinuous Galerkin method for nonlinear convection-diffusion and KdV equations. Computer Methods in Applied Mechanics and Engineering, 2007, 196(37): 3805-3822.
[29] Y. Xu and C.W. Shu. Local discontinuous Galerkin methods for high-order time-dependent partial differential equations, Communications in Computational Physics, 2010, 7: 1-46.
[30] Y. Xu and C.W. Shu. Optimal error estimates of the semidiscrete local discontinuous Galerkin methods for high order wave equations. SIAM Journal on Numerical Analysis, 2012, 50(1): 79-104.
[31] J. Yan and C.W. Shu. A local discontinuous Galerkin method for KdV type equations. SIAM Journal on Numerical Analysis, 2002, 40(2): 769-791.
[32] J. Yan and C.W. Shu. Local discontinuous Galerkin methods for partial differential equations with higher order derivatives. Journal of Scientific Computing, 2002, 17(1-4): 27-47.
[33] N.J. Zabusky and M.D. Kruskal. Interaction of "solitons" in a collisionless plasma and the recurrence of initial states. Physical review letters, 1965, 15(6): 240.
[34] M. Zhang and C.W. Shu. An analysis of three different formulations of the discontinuous Galerkin method for diffusion equations. Mathematical Models and Methods in Applied Sciences, 2003, 13(03): 395-413.